LAPPEENRANTA UNIVERSITY OF TECHNOLOGY

Faculty of Technology

LUT Chemistry

Nikolai Karastelev

MODELING OF HIGH PRESSURE PRETREATMENT PROCESS FOR GOLD LEACHING

Examiners: Professor Ilkka Turunen
D.Sc. (Tech.) Arto Laari

Supervisor: Matti Lampinen
Vladimir Zhukov

ABSTRACT

Lappeenranta University of Technology
Faculty of Technology
LUT Chemistry

Nikolai Karastelev

Modeling of high pressure pretreatment process for gold leaching

Thesis for the Degree of Master of Science in Technology
2013

90 pages, 23 figures, 13 tables and 1 appendix

Examiners: D.Sc. (Tech.) Ilkka Turunen
D.Sc. (Tech.) Arto Laari

Keywords: pretreatment process, pressure oxidation, refractory gold ore and concentrate, leaching, modeling

Investigation of high pressure pretreatment process for gold leaching is the objective of the present master's thesis. The gold ores and concentrates which cannot be easily treated by leaching process are called "refractory". These types of ores or concentrates often have high content of sulfur and arsenic that renders the precious metal inaccessible to the leaching agents. Since the refractory ores in gold manufacturing industry take a considerable share, the pressure oxidation method (autoclave method) is considered as one of the possible ways to overcome the related problems.

Mathematical modeling is the main approach in this thesis which was used for investigation of high pressure oxidation process. For this task, available information from literature concerning this phenomenon, including chemistry, mass transfer and kinetics, reaction conditions, applied apparatus and application, was collected and studied.

The modeling part includes investigation of pyrite oxidation kinetics in order to create a descriptive mathematical model. The following major steps are completed: creation of process model by using the available knowledge; estimation of unknown parameters and determination of goodness of the fit; study of the reliability of the model and its parameters.

ACKNOWLEDGMENTS

I would like to express my sincere gratitude for people who supported and inspired me during working on this Master's Thesis.

I would like to express my appreciation to Professor Ilkka Turunen and D. Sc. Arto Laari for supporting and useful advices.

I owe my special thanks to my friends and colleagues who shared their knowledge and time.

I gratefully acknowledge people who gave me the opportunity to study in Lappeenranta University of Technology and supported me despite the hundreds of miles between us.

TABLE OF CONTENTS

LIST OF SYMBOLS

K_H	Henry's constant, L Pa/mol
k_{O_2}	oxygen mass transfer coefficient, 1/min
n_1	reaction order for pyrite conversion
n_2	reaction order for concentration of dissolved oxygen
n_3	reaction order for pyrite conversion
n_4	reaction order for concentration of ferric ions
P_{O_2}	partial pressure of oxygen in the gas phase, Pa
R	gas constant, R=0.008314 kJ/mol K
r_{O_2}	oxygen mass transfer rate, mol/L min
r_1	surface reaction rate for reaction of pyrite with oxygen, mol / (m^2 min)
r_2	surface reaction rate for reaction of pyrite with ferric ions, mol / (m^2 min)
r_3	reaction rate for reaction of ferrous iron with oxygen, mol/(L min)
T	temperature, K
T_{mean}	mean temperature, K
$[H_2SO_4]$	molal concentration of H_2SO_4, mol/kg H_2O
k_La	volumetric mass transfer coefficient, 1/min
A_i	inner surface area of particle (reactive area), m^2

n	number of solid particles in reactor per liter slurry, 1/L
d_i	inner diameter of particle, m
d_o	outer diameter of particle, m
d_{mean}	mean particle size, m
E_1	activation energy, kJ/mol
E_2	activation energy, kJ/mol
E_3	activation energy, kJ/mol
τ	time for complete conversion of a particle, min
k_1	reaction rate constant
k_2	reaction rate constant
$k_{1,mean}$	reaction rate constant at mean temperature, mol^{n1}/m^{n2} min
$k_{2,mean}$	reaction rate constant at mean temperature, mol^{n1}/m^{n2} min
$k_{3,mean}$	reaction rate constant at mean temperature, mol^{n1}/m^{n2} min
m_{FeS_2}	mass of FeS_2 per liter of slurry, g/L
V_{FeS_2}	volume of pyrite, m^3
V_{slurry}	volume of slurry, L
ρ_{FeS_2}	density of pyrite, g/m^3
x_{FeS_2}	pyrite conversion

c^{*}_{L,O_2}	dissolved oxygen concentration at saturation point, mol/L
c_{L,O_2}	dissolved oxygen concentration, mol/L
c_{FeS_2}	pyrite concentration, mol/L
$c_{FeS_2,0}$	initial pyrite concentration, mol/L
$c_{Fe_{tot}}$	concentration of total dissolved iron, mol/L
$c_{Fe^{3+}}$	concentration of ferric ions, mol/L
$c_{Fe^{2+}}$	concentration of ferrous ions, mol/L
P_{O_2}	oxygen partial pressure, Pa
M_{FeS_2}	molar mass of pyrite, g/mol
ψ	shape factor

INTRODUCTION

Gold is a valuable and highly sought-after precious metal. Nowadays gold industry cannot rely on only high quality gold ores, more often the treatment of gold bearing raw material is accompanied by various difficulties. This class of ore is often termed refractory with the extent of refractoriness that may vary. Direct cyanidation leaching of refractory ores does not often allow achieving gold conversion more than 20%. In addition, reagent consumption can also be prohibitively high. Thereby, there are an increasing number of investigations which concern methods for treatment of refractory gold ores and concentrates.

Sulphide minerals, such as pyrite and chalcopyrite, are the most important sources of value metals. High content of sulfides is usual in refractory gold ores and concentrates. The large amount of sulphur and arsenic renders the valuable metal inaccessible to leaching agents. Since the gold is encapsulated as fine grained particles in the crystal structure of the mineral matrix, such type of gold ore cannot be processed by conventional cyanidation method. Thus, in order to achieve a sufficient recovery, one of the oxidative pretreatment methods such as roasting, pressure oxidation, chlorine-based pressure oxidation, bio-oxidation, and chemical oxidation should be applied.

The commonly used pyrometallurgical method for extraction of gold is flotation with subsequent roasting in the presence of an oxidizing gas, such as air or oxygen, and finally cyanidation of the porous product of roasting. However, increasingly stringent legislation aimed at roaster emissions control for environmental protection worldwide is the reason of higher complexity and costs of the roasting processes.

The oxidative pressure pretreatment process is considered as one of the preparation techniques for the refractory ores. The major developments in the pressure hydrometallurgy of gold ores and concentrates began from the 1980s. The oxidative pretreatment process completely or partially oxidizes the refractory minerals in the ore, rendering gold amenable to cyanide leaching. Although the

process has relatively high capital and operational costs, it is capable to rapid oxidation of the majority of sulfidic and arsenic minerals in the feed and from an environmental point of view, the process is attractive due to production of very small amounts of noxious gases (Marsden, et al., 2006). This method can be used to treat various refractory sulfidic and arsenical ores and concentrates.

There are plenty research in applying this high pressure pretreatment method and consideration of process kinetics. Modeling is one of the approaches which can be used to investigate this poorly known phenomenon. Thus, the aim of this master thesis is to create and apply mathematical models of pressure oxidation process. The following major steps are completed:

- creation of process model by using the available knowledge about the investigated phenomena;
- estimation of unknown parameters and determination goodness of fit;
- study of the reliability of the model and its parameters.

The mathematical model combines the main knowledge about oxidation process, such as chemical kinetics, mass transfer phenomena and the influence of process conditions (impact of temperature, retention time, oxygen partial pressure, and others factors). Modeling is one of the flexible tools of investigation such processes and it is widely used to describe physical and chemical phenomena of pressure oxidation.

Summarizing all that was mentioned above, such aspects of the high-pressure pretreatment process as the role in gold extraction, chemistry, kinetic models and operating conditions are to be considered. The suggested kinetic models should be tested by applying them to experimental data which is collected from literature sources. Finally, the reliability of the model and its parameters should be evaluated.

1 CHEMISTRY OF HIGH-PRESSURE OXIDATION PROCESS

1.1 High-pressure sulfide oxidation under acidic conditions

The composition of the leaching solution in the autoclave industry is dictated by a set of requirements, such as selectivity, availability, relatively low cost of reagent, corrosion of the equipment, and thermal stability (Naboichenko, et al., 2009). Acidic media is the most common condition applied for high-pressure oxidation process. Under strong acidic conditions at temperatures from 100^0C to 170^0C and in the presence of dissolved oxygen, the major oxidation reactions for pyrite (FeS_2), pyrrhotite (Fe_7S_8), arsenopyrite (FeAsS), and chalcopyrite ($CuFeS_2$) are as follows (Marsden, et al., 2006; Holmes, et al., 2000; Bailey, et al., 1976):

$$4FeS_2 + O_2 + 4H^+ \leftrightarrow 4Fe^{2+} + 4S + 2H_2O \quad \text{(R1)}$$

$$2FeS_2 + 2H_2O + 7O_2 \rightarrow 2Fe^{2+} + 4SO^{2-}_4 + 4H^+ \quad \text{(R2)}$$

$$2Fe_7S_8 + 7O_2 + 28H^+ \leftrightarrow 14Fe^{2+} + 16S + 14H_2O \quad \text{(R3)}$$

$$2FeAsS + 5O_2 + 8H^+ \leftrightarrow 4Fe^{2+} + 4HAsO_2 + 4S + 2H_2O \quad \text{(R4)}$$

$$4CuFeS_2 + 3O_2 + 12H^+ \leftrightarrow 4Cu^+ + 4Fe^{2+} + 8S + 6H_2O \quad \text{(R5)}$$

Furthermore, Fe(II) is oxidized to Fe(III) under these conditions (Singer, et al., 1970; Marsden, et al., 2006):

$$4Fe^{2+} + O_2 + 4H^+ \leftrightarrow 4Fe^{3+} + 2H_2O \quad \text{(R6)}$$

Fe(III) is also a strong oxidizing agent and can participate in sulfide oxidation, as follows (Marsden, et al., 2006; Holmes, et al., 2000; Lowson, 1982):

$$FeS_2 + 8H_2O + 14Fe^{3+} \rightarrow 15Fe^{2+} + 2SO^{2-}_4 + 16H^+ \quad \text{(R7)}$$

$$FeS_2 + 4Fe^{3+} + 4O^{2-} \rightarrow 9Fe^{2+} + SO^{2-}_4 + S \quad \text{(R8)}$$

$$FeAsS + 7Fe^{3+} + 4H_2O \leftrightarrow 8Fe^{2+} + AsO^{3-}_4 + 8H^+ + S \quad \text{(R9)}$$

$$CuFeS_2 + 10Fe^{3+} + 4H_2O \leftrightarrow 11Fe^{2+} + Cu^{2+} + 8H^+ + S + SO^{2-}_4 \quad (R10)$$

Thus, ferrous and ferric ions are cycled between the pyrite oxidation reaction (R7) and ferrous ion oxidation reaction (R6). Generally, the rate of oxidation of pyrite rises with concentration of ferric ions, and reduces with concentration of ferrous and H^+ ions (Holmes, et al., 2000). At high temperatures, ferric sulfate typically hydrolyze, resulting in the precipitation of ferric oxide (Fe_2O_3) or basic ferric sulfate ($Fe(OH)SO_4$) depending on acidity (Long, et al., 2004).

The sulfide oxidation reactions (R1), (R8) and (R9) show the formation of elemental sulfur, which can cause problems, as described below (Marsden, et al., 2006):

- coating of sulfide particles by elemental sulfur leading to incomplete oxidation and agglomeration of unreacted sulfide particles;
- coating of exposed gold surface and decreasing of effectiveness of subsequent gold extraction processes;
- consumption of cyanide and oxygen during leaching stage.

Consequently, the formation of elemental sulfur should be avoided. This can be achieved by operating at sufficiently high temperatures (above 170-180^{0}C) which ensures the irreversible oxidation of sulfur to sulfate:

$$2S + 3O_2 + 2H_2O \leftrightarrow 4H^+ + 2SO^{2-}_4 \quad (R11)$$

In practice, temperatures from 180^{0}C to 225^{0}C are used and the overall oxidation reaction equations are (Marsden, et al., 2006):

$$2FeS_2 + 7O_2 + 2H_2O \leftrightarrow 2FeSO_4 + 2H_2SO_4 \quad (R12)$$

$$FeS_2 + 2O_2 \rightarrow FeSO_4 + S \quad (R13)$$

$$2Fe_7S_8 + 31O_2 + 2H_2O \leftrightarrow 14FeSO_4 + 2H_2SO_4 \quad (R14)$$

$$4FeAsS + 13O_2 + 6H_2O \leftrightarrow 4HAsO_2 + 4FeSO_4 \quad (R15)$$

$$4CuFeS_2 + 15O_2 + 2H_2O \leftrightarrow 2Cu_2SO_4 + 4FeSO_4 + 2H_2SO_4 \quad (R16)$$

Bailey and Peters (Bailey, et al., 1976) suggested that oxidation of pyrite is represented by the (R12) and (R13) competing reactions (others authors typically agree with this fact). As the temperature increases, reaction (R12) becomes predominant. The iron, arsenic, and copper species are further oxidized to higher oxidation states: Fe(III) (eq. (R6)), As(V), and Cu(II), respectively (Marsden, et al., 2006).

Any carbonates which are present in the ore react with sulfuric acid:

$$CaCO_3 + H_2SO_4 \leftrightarrow CaSO_4 + CO_2 + H_2O \quad (R17)$$

The carbon dioxide generated decreases the overall efficiency of oxidation by reducing oxygen partial pressure and oxygen utilization.

Nitric acid is also a strong oxidant for refractory sulphide ores and can be used in high-pressure sulfide oxidation processes. High-pressure oxidation of pyrite by nitric acid is described by the following equations (Developments in the pretreatment of refractory gold minerals by nitric acid, 2009):

$$2FeS_2 + 10HNO_3 = H_2SO_4 + Fe_2(SO_4)_3 + 10NO + 4H_2O \quad (R18)$$

$$2FeAsS + 8HNO_3 + H_2SO_4 = Fe_2(SO_4)_3 + 2H_3AsO_4 + 8NO + 2H_2O \quad (R19)$$

$$2NO + O_2 = 2NO_2 \quad (R20)$$

$$3NO_2 + H_2O = 2HNO_3 + NO \quad (R21)$$

$$4FeS_2 + 15O_2 + 2H_2O = 2H_2SO_4 + 2Fe_2(SO_4)_3 \quad (R22)$$

The similar chemistry can be suggested for any sulphide mineral. As can be seen, the nitric oxide gas which was produced according Equations 18 and 19 is further oxidized. Nitrogen dioxide is absorbed by water at high pressure thereby regenerate the nitric acid (Developments in the pretreatment of refractory gold minerals by nitric acid, 2009). Equation 17 shows the overall reaction. The nitric

acid is present as a catalyst and is not consumed. Thus, pressure oxidation of pyrite involves a number of consecutive and/or parallel reactions which results in formation of ferrous and ferric ion, sulphate ion and elemental sulphur as products. The presence of the various products depends on the applied conditions, such as time, temperature, partial pressure of oxygen, acidity, and total sulphate concentration. The level of impact of the mentioned parameters is discussed in Chapter 2.4.

1.2 High-pressure sulfide oxidation under neutral/alkaline conditions

The autoclave oxidation process can be carried out not only in acidic media, but also under alkaline and neutral conditions. In neutral and alkaline conditions at the presence of dissolved oxygen, pyrite (FeS_2), pyrrhotite (Fe_7S_8), arsenopyrite (FeAsS), and chalcopyrite ($CuFeS_2$) are oxidized as follows (Marsden, et al., 2006):

$$4FeS_2 + 15O_2 + 14H_2O \leftrightarrow 4Fe(OH)_3 + 16H^+ + 8SO^{2-}_4 \quad \text{(R23)}$$

$$4Fe_7S_8 + 69O_2 + 74H_2O \leftrightarrow 28Fe(OH)_3 + 64H^+ + 32SO^{2-}_4 \quad \text{(R24)}$$

$$2FeAsS + 7O_2 + 8H_2O \leftrightarrow 2Fe(OH)_3 + 2H_3AsO_4 + 4H^+ + 2SO^{2-}_4 \quad \text{(R25)}$$

$$4CuFeS_2 + 17O_2 + 18H_2O \leftrightarrow 4Cu(OH)_2 + 4Fe(OH)_3 + 16H^+ + 8SO^{2-}_4 \quad \text{(R26)}$$

Investigations of the possibility to use alkaline pressure oxidation as a way to prepare gold concentrates with high content of arsenic for cyanidation show that oxidation of sulfide gold minerals in alkaline media can be carried out under significantly milder conditions than in acidic media (Non-ferrous metallurgy, 1967). Sulfur and arsenic are almost completely transferred into the solution in the form of sulfate and arsenate ion. Elemental sulfur is not formed. The subsequent cyanide leaching of the oxidation residues generally gives high recovery of gold. Alkaline solutions have a low corrosive activity. Therefore, inexpensive

construction materials can be used for the manufacturing of the autoclave equipment. The advantages of alkaline method are the absence of the acidic ore processing operations, rinsing and neutralization of the leached pulp and savings in acid and lime. However, despite the advantages, the application of alkaline method is practically rare due to high consumption of expensive lime, and lack of simple methods for regeneration of chemicals. Additional difficulties arise from obtaining the arsenic in a form convenient for disposal.

Nonacidic pressure oxidation employs similar conditions of pressure, temperature, and oxygenation to the acidic process, but neutral or slightly alkaline pH is applied (Marsden, et al., 2006). This method can be used for the treatment of refractory ores which contains large amounts of acid-consuming carbonates and has low sulfide content and therefore less suitable to acidic oxidation. Thereby, acid is not added into the process, and generated acid is neutralized by carbonates in the feed. “Mercur” (see the Table 4.1) is the only gold mining company which has applied pressure oxidation in neutral (slightly alkaline) conditions. Due to low content of sulfides (1-1,5% sulfide sulfur) and unusually high content of carbonates (about 20%), high amount of acid is needed in the acidification stage. Thus, autoclave oxidation of sulfide gold minerals can be efficiently carried out in acidic or nearly neutral environments.

2 PHENOMENA IN HIGH-PRESSURE OXIDATION PROCESS

2.1 Overview of process phenomena

It is clear that fluid-solid reactions have a considerable role in hydrometallurgical processes and, as a tool of investigation of heterogeneous reactions in which a gas or liquid contact and react with a solid material, different kinetic studies have been carried out by Papangelakis and Demopoulos (1989), Long and Dixon (2003) and other researchers. The success of the high-pressure oxidation pretreatment process as a real alternative for mineral treatment has motivated researchers to develop mechanistic models for simulation and optimization of this process.

High pressure hydrometallurgical reactors for pretreatment of gold ores and concentrates are complex 3-phase systems, which include dissolution and precipitation reactions that are mainly dependent on the solution chemistry, temperature and vessel pressure (Baldwin, et al., 1998). The chemical reactions taking place during the pressure oxidation process are controlled by inherent chemical reaction kinetics and the rate of mass transport of each reacting species between gas, liquid and solid phases.

The phenomena which appear as a result of interactions of reactants in a 3-phase system were described by Yagi and Kunii (1955, 1961) as part of the shrinking core kinetic model (SCM) of noncatalytic heterogeneous reaction. The shrinking core model considers several consecutive steps taking place during the heterogeneous chemical reaction and can be used as a way to represent the basic phenomena in pressure oxidation process.

According to the shrinking-core model, the reaction proceeds in a narrow front which moves into the solid particle, leaving behind completely converted material and inert solids (Levenspiel, 1999). This means that at any time there exists an unreacted core of material which shrinks in size during the reaction, leaving

behind reacted and inert solids which is called "ash". Thus, while the reaction proceeds there always exists an unreacted core of material which shrinks in size, as shown in Figure 2.1. A complete picture of pressure oxidation can be obtained by taking into account the oxygen mass transfer into bulk liquid surrounding the solid particles and the subsequent oxidation of the solid particles.

Thereby, the major steps in a pressure oxidation process are presented as follows (Marsden, et al., 2006; Levenspiel, 1999):

- *stage 1*: mass transport (dispersion and dissolution) of gaseous reactants (oxygen) into the solution phase (Figure 2.1. Pos. 1 and 2);
- *stage 2*: mass transport of the reacting species (dissolved oxygen) through the solution-solid boundary layer to the surface of the solid mineral (Figure 2.1. Pos. 3);
- *stage 3*: chemical (or electrochemical) reaction at the solid surface (Figure 2.1. Pos. 4-7). This stage usually includes several sub stages:
    - surface hydroxylation-hydration;
    - reaction of surface species;
    - adsorption of reacting species onto the solid surface;
    - desorption of product species from the solid surface;
    - reaction of product in the solution;
- *stage 4*: mass transport of the reaction product through the boundary layer into the bulk solution (Figure 2.1. Pos. 8).

The resistance of the different steps can vary considerably. In the case of the overall reaction rate is determined by stages 1, 2, or 4, the reaction is controlled by mass transport. The reaction is said to be chemically controlled if the stage 3 limits the rate.

According to the above mentioned phenomena, the block diagram in Figure 2.2 represents the full picture of the pressure oxidation process when autoclave is used as the reactor (see Chapter 4.2). This block diagram takes into account all the

input and output flows and shows the various phenomena as a result of the interaction between the different phases.

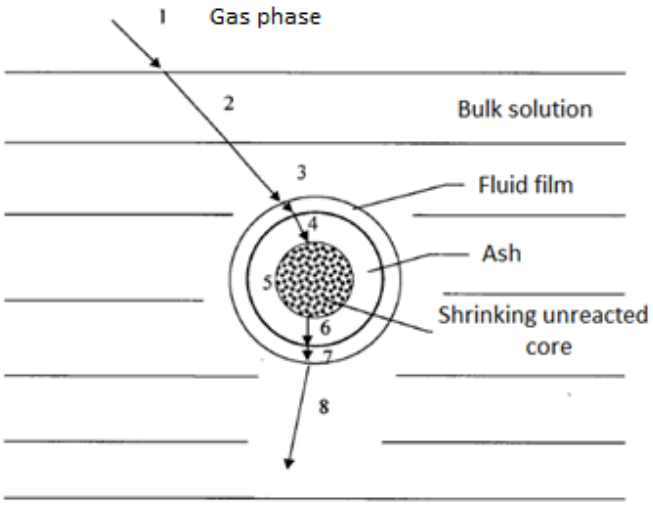

Figure 2.1 Schematic diagram of shrinking core model (SCM).

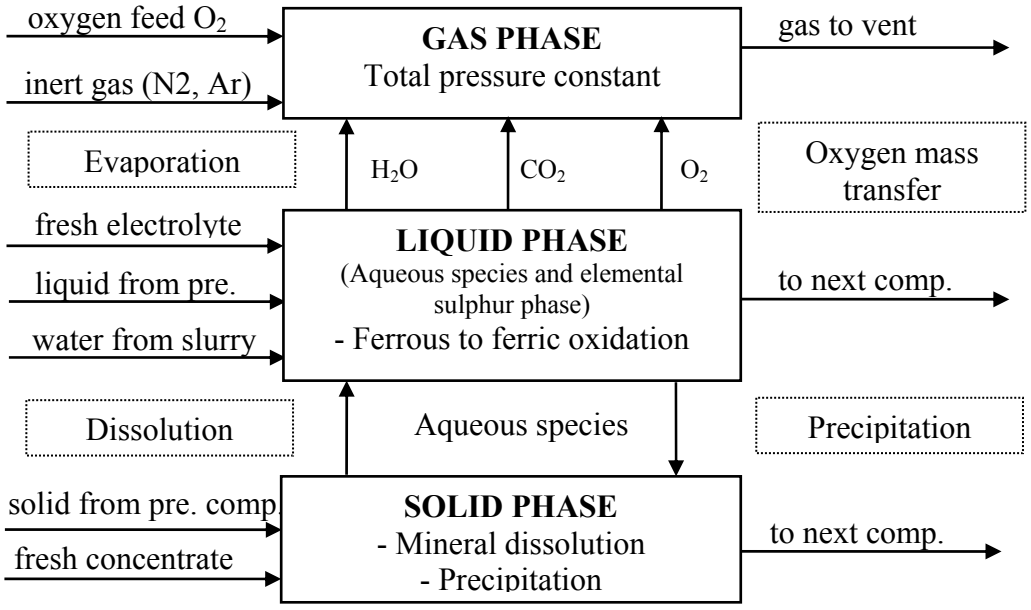

Figure 2.2 Block diagram of the inputs and outputs for the pressure oxidation process (Baldwin, et al., 1998).

2.2 Kinetics of the sulfide oxidation

2.2.1 Kinetics of sulfide dissolution

The interaction of sulfides with acidic and alkaline solutions in the presence of various reagents such as oxidants, complexing agents, and surfactants compounds is widely discussed in various publications. Generally, the dissolution of sulphide minerals is explained by two mechanisms: hydrolytic (non-oxidative) and oxidative.

Hydrolytic mechanism is usually observed for metal's monosulfides (such as ZnS), as follows (Lucik, et al., 2009):

$$MeS + 2H^{+} = Me^{2+} + H_2S \qquad \text{(R27)}$$

Oxidative dissolution of sulfide can be a chemical or electrochemical process (Nowak, 2001). Oxidation of metal sulfides is a multi step process which includes intermediate compounds acting as catalysts or inhibitors for the other stages.

Chemical dissolution follows the scheme (Lucik, et al., 2009):

$$\begin{array}{l} MeS \rightarrow Me^{2+} + S^{2-}; \qquad S_8 \\ \qquad\qquad\quad \downarrow \qquad\quad \uparrow \\ \qquad\qquad\quad HS^{-} \rightarrow HS_n^{-} \rightarrow S_2O_3^{2-} \rightarrow SO_4^{2-} \rightarrow in\ solution \end{array} \qquad \text{(R28)}$$

Oxidation of sulphide sulfur proceeds stepwise, and in acidic solutions by the following scheme (Sato, 1960):

$$S^{2-} \rightarrow S \rightarrow SO_4^{2-} \qquad \text{(R29)}$$

Electrochemical reactions are caused by electron transfer. Electrochemical dissolution can be presented by the following scheme (Lucik, et al., 2009):

$$\begin{array}{ccccccc} in\,solution & & & & S_2O_3^{2-} \rightarrow SO_4^{2-} \rightarrow in\,solution & & \\ \uparrow & & & & \uparrow & & \\ Me_kS_m \rightarrow Me^{2+} + 2\overline{e} + Me_{k-1}S_m & \rightarrow & Me_{k-1-x}S_m + 2x\overline{e} + xMe^{2+} & & & & \text{(R30)} \\ \uparrow & & \downarrow & & \downarrow & & \\ \leftarrow - - - Me_{k-1}S_m + S_8 & & in\,solution & & & & \end{array}$$

Electrochemical dissolution includes two coupled reactions: cathodic reduction of an oxidant and an anodic oxidation of sulfide. Reduction of O_2 occurs via the formation of H_2O. Anodic dissolution typically takes place via the formation of the metal-sulfide, which can turn into a lower sulphide (if one exists) or into original sulphide with formation of sulfur and stoichiometric sulfide (Lucik, et al., 2009).

2.2.2 Kinetics of pyrite dissolution

Interest in the kinetics and mechanism of pyrite oxidation relates to the fact that pyrite is the most common sulphide. The pyrite does not have economic importance and is generally viewed as a gangue mineral, but pyrite often influences the recovery of associated metal values such as gold, zinc, and copper (Long, et al., 2004). Thus, pyrite oxidation has been studied extensively because of its significance in areas such sulfide mineral separations by floatation, the generation of acid in mine waters and leaching processes.

In many cases it is reported that the oxidation of pyrite comprises the following products: ferrous sulfate, ferric sulfate, sulfuric acid and elemental sulfur. But the possible pathways of the aqueous oxidation of pyrite and explanation of reaction mechanism could be slightly different. Concerning pressure oxidation process, two mechanisms are discussed: oxidation through a sequence of chemical reaction, and oxidation through an electrochemical reaction (Lowson, 1982).

The discussions of common *chemical reactions* of pyrite oxidation in acidic and neutral media were introduced above (see Chapter 1.1 and 1.2). Generally, pyrite oxidation can be presented by using three main equations (Papangelakis, et al., 1992; Long, et al., 2004; Holmes, et al., 2000):

$$FeS_{2(s)} + 7/2O_{2(aq)} + H_2O \rightarrow FeSO_{4(aq)} + H_2SO_{4(aq)} \quad \text{(R31)}$$

$$FeS_{2(s)} + 7Fe_2(SO_4)_{3(aq)} + 8H_2O \rightarrow 15FeSO_{4(aq)} + 8H_2SO_{4(aq)} \quad \text{(R32)}$$

$$2FeSO_{4(aq)} + 1/2O_2 + H_2SO_{4(aq)} \rightarrow Fe_2(SO_4)_{3(aq)} + H_2O \quad \text{(R33)}$$

The kinetics of reactions, which are represented by Equation (R31) and (R32), can be described by above mentioned shrinking core model (SCM) model. Generally, the shrinking core model (SCM) gives reasonable kinetic equation which describes the conversion of solid component. SCM can take into account possible rate control cases: the SCM controlled by chemical reaction or the SCM controlled by diffusion trough the solid product layer (Levenspiel, 1999). The suggested conversion versus time equation for the possible rate limitation cases are presented in Table 2.1. In general, most of suggested kinetics of pyrite conversion is variations of SCM model.

The rate of homogeneous oxidation of ferrous ion to ferric ion (Equation (R33)) can be represented by using general expression (Papangelakis, et al., 1991; Baldwin, et al., 1998):

$$\frac{dc_{Fe^{2+}}}{dt} = k_1 c_{Fe^{2+}}^2 c_{L,O_2} \quad (1)$$

where k_1 - reaction rate constant

$c_{Fe^{2+}}$ - concentration of ferrous ions, mol/L

c_{L,O_2} - dissolved oxygen concentration, mol/L

Table 2.1 SCM model expressions for various rate-controlled situations (Levenspiel, 1999).

	Small Particle (Stokes regime)	Large particle (u = constant)
Film Diffusion Controls	$\frac{t}{\tau} = 1-(1-X)^{2/3}$ $\tau = \frac{\rho R_0^2}{2bDC_A}$	$\frac{t}{\tau} = 1-(1-X)^{1/2}$ $\tau = \frac{R_0^{3/2}}{C_A}$
Ash Diffusion Controls	Not applicable	Not applicable
Reaction Controls	$\frac{t}{\tau} = 1-(1-X)^{1/3}$ $\tau = \frac{\rho R_0}{bkC_A}$	$\frac{t}{\tau} = 1-(1-X)^{1/3}$ $\tau = \frac{\rho R_0}{bkC_A}$

* where τ - the time required for complete conversion; t - time; X - fraction conversion of reacted mineral; ρ - the density of the mineral; C_A - the reactive concentration in the solution; R_0 - the radius of the un-reacted particle; b - the stoichiometry coefficient according reaction *A(fluid)* + *bB(solid)* → *products*; k - the first-order rate constant for the surface reaction.

The dissolution kinetic of pyrite due to an *electrochemical mechanism* is one of the probable theories which were discussed by several researchers (Holmes, et al., 2000; McKibben, et al., 1986; Williamson, et al., 1984). According this theory, the dissolution of pyrite is described by an oxidation-reduction reaction since the pyrite is oxidized and the ferric ions and oxygen are reduced at the pyrite surface. The overall reaction could be written in terms of the half reactions for the oxidation of pyrite and the reduction of ferric ions (Holmes, et al., 2000).

The first half-reaction is the anodic oxidation of pyrite:

$$FeS_2 + 8H_2O \rightarrow Fe^{2+} + 2SO^{2-}{}_4 + 16H^+ + 14e^- \qquad \text{(R34)}$$

The cathodic reduction of ferric ions or dissolved oxygen is the second half-reaction:

$$Fe^{3+} + e^{-} = Fe^{2+} \quad \text{(R35)}$$

$$O_2 + 4H^{+} + 4e^{-} \rightarrow 2H_2O \quad \text{(R36)}$$

It should be noticed that the reaction (R34) is referred to as the anodic dissolution of pyrite, while reaction (R2) and (R7) is referred to as the oxidative dissolution of pyrite. The investigation of rate of the reaction (R34), (R35), and (R36) is based on the exponential dependence on the potential across the mineral-solution interface. Since driving force of electrochemical reactions is a potential (voltage) difference, the nascent flow of electrons (or an electrical current) could be accurately measured directly. Hence, the rate of electrochemical reactions can be quantified much easily (Marsden, et al., 2006). Holmes and Crundwell (Holmes, et al., 2000) investigated reactions given by equations (R34), (R35) and (R36) separately since they occur independently. That means, the rate expression for individual half-reaction was established.

The empirical rate equations that have been proposed for the oxidative dissolution of pyrite by dissolved iron and oxygen are given in Table 2.2 and Table 2.3 respectively. According the model of Garrels and Thompson (1960) and Lowson (1982), the rate does not depend on concentration of $[Fe^{3+}]$ in the absence of the ferrous ions. That conclusion could be wrong since dissolution of pyrite requires an oxidizing agent. Holmes and Crundwell (1999) and McKibben and Barnes (1986) obtain a similar order by Fe^{3+} and H^{+}. The half-order reaction rate of pyrite dissolution of oxygen seems most probable according to the reported expression of the pyrite reaction rate in solution containing dissolved oxygen.

Table 2.4 shows the experimental conditions, orders of reaction for oxygen partial pressure, and obtained activation energies from several studies on pressure oxidation of pyrite in acid media. Generally, authors indicate that the reaction orders for oxygen partial pressure depend on both temperature and pressure.

Table 2.2 Rate expression for the dissolution of pyrite in solution containing dissolved iron (Holmes, et al., 2000).

Rate expression	Reference
$r_{FeS_2} = k \cdot [Fe^{3+}] / \sum [Fe]_i$	Garrels and Thompson (1960)
$r_{FeS_2} = \frac{k_1 \cdot [Fe^{3+}]^{0.5} - k_2 \cdot [Fe^{2+}]^{0.5}}{1 + k_3 \cdot [Fe^{3+}]^{0.5} + k_4 \cdot [Fe^{2+}]^{0.5}}$	Smith and Shumate (1970)
$r_{FeS_2} = k \cdot [Fe^{3+}] \cdot [H^+]^{-0.44} / \sum [Fe]_i$	Mathews and Robins (1972)
$r_{FeS_2} = k \cdot [Fe^{3+}] \cdot [Fe^{2+}] / \sum [Fe]_i$	Lowson (1982)
$r_{FeS_2} = k \cdot [Fe^{3+}]^{0.58} \cdot [H^+]^{-0.5}$	McKibben and Barnes (1986)
$r_{FeS_2} = k \cdot [Fe^{3+}]^{0.3} \cdot [Fe^{2+}]^{-0.47} \cdot [H^+]^{-0.32}$	Williamson and Rimstidt (1994)
$r_{FeS_2} = k [H^+]^{-0.5} \left(\frac{k_{Fe^{3+}} [Fe^{3+}]}{k_{FeS_2} [H^+]^{-0.5} + k_{Fe^{2+}} [Fe^{2+}]} \right)^{0.5}$	Holmes and Crundwell (1999)

Table 2.3 Rate expression for the dissolution of pyrite in solution containing dissolved oxygen (Holmes, et al., 2000).

Rate expression	Reference
$r_{FeS_2} = k \cdot [O_2]^{0.81}$	Mathews and Robins (1974)
$r_{FeS_2} = k_1 \cdot \left(\frac{[O_2]}{k_2 + [O_2]} \right)^{0.5}$	Bailey and Peters (1976)
$r_{FeS_2} = k \cdot [O_2]^{0.5}$	McKibben and Barnes (1986)
$r_{FeS_2} = k \cdot [O_2]^{0.5} \cdot [H^+]^{-0.11}$	Williamson and Rimstidt (1994)
$r_{FeS_2} = k \cdot [O_2]^{0.5} \cdot [H^+]^{-0.18}$	Holmes and Crundwell (1999)

One-half order dependence corresponds to higher oxygen partial pressures and temperature while first-order dependence is exhibited predominantly at lower pressure (< 20 atm) and at various temperatures. Activation energies are slightly different, but mostly in range of 46 and 55 kJ/mol at temperature below 160^0C, and 50-80 kJ/mol as the temperature higher than 160^0C. The activation energy of 110.5 kJ/mol which is reported by Papangelakis and Demopoulos (Papangelakis, et al., 1991), is questioned by many authors. Finally, these values can be good starting points during parameters estimation procedure.

Table 2.4 Review of pyrite pressure oxidation kinetic studies (Papangelakis, et al., 1991; Long, et al., 2004).

Material	**Experimental conditions**			**P_{O2} order**	**Activation energy, kJ/mol**	**Assumed mechanism**	**Ref.**
	H_2SO_4 M	**T, ^{0}C**	**P_{O2}, atm**				
Natural pyrite	0	130-210	2.7-14.0	0.5	83.7	Surface controlled, chemisorption	Warren and Austr, 1956
Upgraded pyrite concentrate	0	130-165	6.1-23.8	0.5	70.3-77.4	Chemical control	Cornelius and Woodcock, 1958
Upgraded pyrite concentrate	0.075	100-130	0-4	1	55.7	Chemisorption chemical reaction	McKay and Halpern, 1958
Natural pyrite	0.2	60-130	0-15.5	1	54.8	Chemisorption chemical reaction	Gerlach et al., 1966
Natural pyrite	1.0	85-130	0-20	1	51.1	Electrochemical reaction	Bailey and Peters, 1976
			20-66.4	0.5			
Natural pyrite	0.5	140-160	5-20	1	46.2	Electrochemical reaction	Papangelakis and Demopoulos, 1991
		160-180	5-20	1	110.5		
		160-180	10-20	0.5			

2.3 Oxygen mass transfer

Oxygen usually is supplied to the first several compartments as bubbles of gas directly under mixing agitator. Generally, the oxygen absorption rate is a function of several factors: surface area of the liquid, superficial velocity of gas bubbles, temperature, degree of agitation, partial pressure of the gas, liquid viscosity, and concentration of dissolved gas and other species.

The oxygen mass transfer rate can be simply determined using the following equation:

$$r_{L,O_2} = k_L a(c^*_{L,O_2} - c_{L,O_2})[mol / L_{liq} \text{ min}] \quad (2)$$

where $k_L a$ - the mass transfer coefficient times the specific surface area of the oxygen bubbles, 1/min

c_{L,O_2} - dissolved oxygen concentration, mol/L

c^*_{L,O_2} - dissolved oxygen concentration at saturation point, mol/L

The parameter $k_L a$ is determined by model parameters estimation procedure. Dependence of molar saturation concentration of dissolved oxygen on the oxygen partial pressure can be evaluated in two ways:

- Henry's law:

$$c^*_{L,O_2} = K_H \, P_{O_2} \; [mol / L_{liq}] \quad (3)$$

where c^*_{L,O_2} - dissolved oxygen concentration at saturation point per liter of liquid phase, mol/L

K_H - Henry's constant, L Pa/mol

P_{O_2} - partial pressure of oxygen in the gas phase, Pa

- Tromans (1998) model (see Figure 2.3) for dissolved oxygen concentration is:

$$c^*_{L,O_2} = 101325\,\psi \exp\left(\frac{-0.046T^2 + 203.35T\ln T - 1430.55T + 68669}{8.3143T}\right) P_{O_2}\ [mol/L_{liq}] \quad (4)$$

where c^*_{L,O_2} - dissolved oxygen concentration at saturation point per liter of liquid phase, mol/L

T - temperature, K

P_{O_2} - partial pressure of oxygen in the gas phase, Pa

ψ - concentration-dependent parameter, in case of sulfuric acid alone in molar concentration units this coefficient is expressed as:

$$\psi = \left(\frac{1}{1 + 2.01628\,[H_2SO_4]}\right)^{0.168954} \quad (5)$$

where $[H_2SO_4]$ - molal concentration of H_2SO_4, mol/kg H_2O

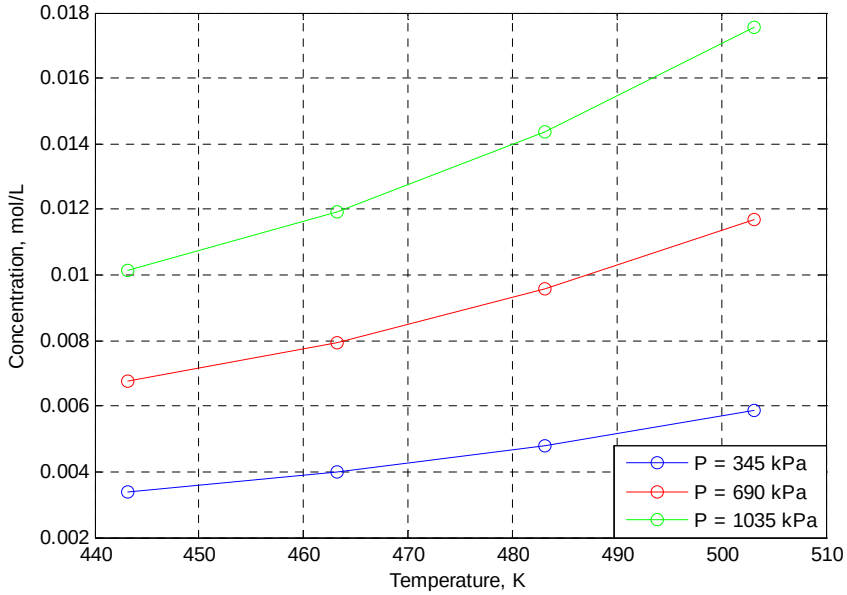

Figure 2.3 Concentration of dissolved oxygen at various temperatures and pressures by using Tromans (1998) model.

2.4 Variables affecting the phenomena

As was discussed above, the pressure oxidation of pyrite involves a number of consecutive and/or parallel reactions which yield ferrous (Fe^{2+}) and ferric (Fe^{3+}) ion, sulphate ion (SO_4^{2-}) and elemental sulphur (S_0) as products. The relative abundance of the various products formed depends on the applied conditions, namely:

- temperature and pressure of oxygen (air);
- acid concentration and pH;
- degree of agitation;
- pulp density;
- particle size;
- residence time.

Let's consider the impact of these variables to oxidation kinetic by taking into account the kinetic of the oxidation process, mass transfer, some economic aspects, and process limitations.

2.4.1 Temperature and oxygen pressure

The oxidation rate generally increases with growing temperature (Papangelakis, et al., 1991; Long, et al., 2004; Holmes, et al., 2000). Increase in the oxygen pressure increases the rate of oxidation processes, which provides a more complete oxidation of sulphides, arsenides, and metal ions. The elemental sulphur formation is a phenomenon which is strongly depends on temperature. As reported, at the temperature lower than 160^0C, elemental sulphur formation blocks the grain surface, thereby, terminates the oxidation reaction before complete conversion of pyrite is achieved (Papangelakis, et al., 1991). At the same time, temperatures higher than 160^0C allow to complete the reaction without any hindrance.

However, the pressure also rises at higher temperatures. This fact leads to complexity and higher costs in the design and operation of the oxidation process at higher temperatures. For instance, oxidation at 250 ^{0}C requires operating pressures of about 6200 kPa. The upper limit of temperature and pressure is constrained by several issues: mechanical limitations (e.g. seals); increasing aggressiveness of the medium; increasing capital and operating costs; increasing steam consumption; exothermic reactions of oxidative process. The operating temperature and pressure are typically maintained at minimal sufficient level to avoid formation of elemental sulfur and to provide the desired oxygen partial pressure for effective sulfide mineral oxidation (Marsden, et al., 2006).

2.4.2 Acid concentration and pH

The acid concentration is selected considering the following factors depending on the composition of the raw material (e.g. presence of acid consumers and sulfur content): to maintain sufficient free acid to retain iron species in the solution; to avoid excessive precipitation; to sustain satisfactory oxidizing potential; to have tolerable costs of further neutralization. Generally, acid concentration is retained above 10 g/L H_2SO_4 (Marsden, et al., 2006).

2.4.3 Degree of agitation

Sufficient degree of agitation is needed to provide satisfactory heat and mass transfer in the autoclave. The absorption rate of oxygen into the liquid phase also depends on the mixing conditions because the increase of agitation intensity leads to higher dispersion and retention of oxygen bubbles in the slurry. The agitation intensity is, however, limited by a number of factors such as high energy costs, construction problems, possible foaming, and erosion and cavitation problems.

Experiments conducted by Hu Long and David G. Dixon show that agitation speed had no considerable effect on the initial rate of pyrite oxidation when agitation maintained higher than 800 rpm (Long, et al., 2004).

Finally, such characteristics as the reactor and impeller design, density and viscosity of the slurry, mixing power and impeller tip speed impact on the degree of agitation. Typically, radial flow multi blade impellers (for example Rushton turbine) are applied, but other alternative impeller designs are also possible (Marsden, et al., 2006).

2.4.4 Pulp density

The optimal value of the pulp density is mainly a compromise between minimizing the size of the reactor by maximizing the pulp density and maximizing the mass transfer of oxygen. The high slurry density leads to increase in the productivity (especially in case of poor ores), but mass transfer conditions deteriorate and the load on the mixing device is increased. Long and Dixon (Long, et al., 2004) indicate that increasing pulp density has a beneficial effect on the rate of pyrite oxidation.

The formation of sulfur products such as elemental sulfur and ore characteristics can also influence the selection of the operating slurry density. The formation of sulfur is usually not a problem in case of low-sulfide sulfur ores and slurry densities from 45% to 55% are appropriate. Slurry with high sulfur content, such as flotation concentrate, should be treated at lower density, usually 30% to 40% of solids (sometimes 10% to 15%), or part of the product should recycled (Marsden, et al., 2006). Typically, lower slurry densities are used for ores and concentrate which are richer. Low density may be also required in cases when the ores contain carbonates (to avoid formation of gypsum) or have high clay content (to maintain the operating density of the slurry).

2.4.5. Particle size

Small particle size leads to increasing sulfide surface area. Small particles have therefore higher oxidation rates with shorter reaction residence time and higher degree of oxidation. The optimum particle size is determined by comminution costs, costs of extended oxidation residence time, and the degree of oxidation

required. However, overgrinding the material is energy intensive and difficulties might appear in the separation and clarification of the solutions. Fine grinding can also increase foaming, which reduces the efficiency of the reaction volume in the autoclave (Naboichenko, et al., 2009). In pressure oxidation of ores, materials are typically grinded to 70% to 80% < 75μm (Marsden, et al., 2006) or 80%-90% < 64 μm (Naboichenko, et al., 2009), whereas pressure oxidation of concentrates usually treats a finer material between 70% to 80% < 37μm (Table 4.1).

2.4.6 Residence time

The residence time required to obtain the demanded conversion depends essentially on temperature and pressure of the reaction mixture, intensity of mixing and slurry properties, such as type and amount of sulfide minerals presented and the particle size of material. Residence time of between 1 and 2 hours are generally necessary. Longer residence times are less feasible since of the potentially higher capital and operating costs of the process (Marsden, et al., 2006). Any reduction that can be achieved in residence time leads to higher autoclave performance or require less its reaction volume.

3 REFRACTORY GOLD ORE TREATMENT

3.1 Refractory gold ores and concentrates

Gold is widely distributed in nature due to its physical and chemical properties. It is present in lithosphere (crust, mantle of the earth), hydrosphere (sea water), and biosphere (flora). Possible sources of gold for extractive metallurgy are alluvial and placer deposits, veins associated with quartz and various sulfide minerals. The term "refractory gold ore" is often used when the difficulties in treatment such kind raw material emphasized. In hydrometallurgy of gold the extraction process of metal from ores and concentrates can be generalized by three basic procedures (Derry, 1972):

- dissolution of valuable compounds or metals from an ore or concentrate into a leach solution;
- purification and upgrading of the leach solution;
- recovery of the valuable components from the purified solution.

In most cases the above mentioned difficulties in refractoriness appear during the dissolution of the ore or concentrate by various leaching agents. The amount of gold which can be extracted by the leaching process determines the economic feasibility. It mainly depends on the type of the used ores. According to different literature sources the most often mentioned reasons for gold refractoriness are:

- Gold is locked in reactive gangue minerals (often sulfide, such as pyrite and arsenopyrite) and cannot be adequately liberated, even after fine grinding. In this case, the refractoriness can be explained by the dissemination of fine grained or submicroscopic gold inclusions within sulphide minerals such as arsenopyrite and pyrite (Marsden, et al., 2006). Because of this, such ores require a pretreatment process to modify or destroy the sulphide matrix to render the gold accessible to cyanide and oxygen (Gudyanga, et al., 1999).

- Gold appear with minerals that consume too much reagents. These minerals are, for example, pyrrhotite, marcasite, and arsenopyrite (Marsden, et al., 2006).
- Gold occurs with carbonaceous materials that allow cyanide to dissolve gold but quickly adsorb gold back on the active carbon in the ore (Marsden, et al., 2006).
- Gold is associated with tellurides (Leons Eugene, et al., 2009).
- Gold or silver is contained in base metal sulfides of lead, copper and zinc (Leons Eugene, et al., 2009). The high content of copper and zinc requires uneconomically high quantities of cyanide to process the ore due to the solubility of copper and zinc in cyanide solutions.
- Various combinations of the cases mentioned above is also possible.

Lodejshhikov (1999) suggested that the main factor for characterization of gold and silver refractory ores is the recovery factor at the leaching stage:

$$K_e^c = 1 - (K_p + K_h + K_s) \qquad (6)$$

The meaning of the various coefficients is:

- K_p - physical dispersion coefficient characterizing the relative proportion of dispersed gold associated with dense and insoluble minerals in the leaching solutions.
- K_h - chemical dispersion coefficient which take into account the influence of impurities, such as the oxidized sulphide minerals of copper, iron, antimony, arsenic, zinc, lead and other impurities. The negative impact of the impurities decrease the concentration of active cyanide (during cyanidation process) in liquid phase and increases cyanide consumption.

- K_s - sorption activity of ore characterizing the negative influence of the mineral complex on gold recovery in leaching process due to adsorption of dissolved metals by the ore.

The coefficients K_h and K_s, in contrast to K_p, are not constant for the same material and can vary in wide limits depending on the conditions of cyanidation process. These three coefficients can be determined experimentally and serve for assessment of gold ore refractoriness.

The reasons for the gold refractoriness show that the composition of ore/concentrate has a significant role. Some of the gold-bearing minerals and associated host minerals, such as iron oxides, silicates and carbonates, carbonaceous material, sulfides, and sulfosalts, are shown in Table 3.1.

According Table 3.1 it can be concluded that the sulphide minerals are one of the most important sources of value metals, such as gold, copper, silver, and zinc. Among the various kinds of gold ores and concentrates, the proportion of sulfide and carbonaceous sulfide gold ore with pyrite-arsenopyrite mineralization is estimated to be about 30-40% of the total world reserves of gold (Lodejshhikov, 2008). The interest of many researchers in developing methods for successful processing such raw materials is obvious. Arsenopyrite (FeAsS) and pyrite (FeS_2), which are commonly present in gold ores, do not allow to leach gold with efficiencies more than 50%. Thus, a pretreatment process prior to leaching is required.

Table 3.1 Some of gold-bearing and host minerals (Gasparrini, 1983; Boyle, 1980; Vaughan, 2004).

	Mineral	Formula	
	Gold-bearing minerals		
	Native gold	Au	
	Electrum	(Au, Ag)	
Alloy	Cuproauride	(Au, Cu)	
	Porpezite	(Au, Pd)	
	Rhodite	(Au, Rh)	
	Iridic gold	(Au, Ir)	
	Platinum	(Au, Pt)	
	Bismuthian gold	(Au, Bi)	
	Maldonite	(Au2Bi)	
	Auricupride	(AuCu3)	
Tellurides	Calaverite	(AuTe2)	
	Krennerite	(Au, Ag)Te2	
	Montbrayite	(Au, Sb)2Te3	
	Petzite	(Ag3AuTe2)	
	Muthamannite	(Ag,Au)Te	
	Sylvanite	(Au, Ag)Te4	
	Kostovite	(AuCuTe4)	
	Compounds		
	Host minerals for gold		Gold Concentration*
Sulfides and Sulphosalts	Pyrite	FeS2	< 0,25-800 ppm
	Arsenopyrite	FeAsS	< 0,3 ppm-1,7 wt.%
	Loellingite	FeAs2	1,5-1,087 ppm
	Chalcopyrite	CuFeS2	0,01-20 ppm
	Orpiment	As2S3	[no data]
	Realgar	As2S2	[no data]
	Stibnite	Sb2S3	[no data]
	Jamesonite	2PbS,Sb2S3	[no data]
	Chalcocite	Cu2S	[no data]
	Galena	PbS	[no data]
	Sphalerite	ZnS	[no data]
	Linnaeite	Co3S4	[no data]
	Molybdenite	MoS2	[no data]
	Marcasite	FeS2	0,05-4,1 ppm
	Tetrahedrite	(Cu,Fe)12Sb4S13	< 0,25-59 ppm
	Antimony-arsenic-bismuth-lead suphosalts		
Oxides	Quartz	SiO2	
	Magnetite	Fe3O4	
	Secondary iron oxides		
	Silicates and carbonates		
	Carbonaceous materials		

* 1ppm = 1g/t

3.2 Role of pretreatment processes

History of metallurgical methods of gold recovering began from gravity separation and amalgamation, which were gradually replaced by more profitable processes such as cyanidation. Actually there are no dramatic changes in the metallurgical techniques for gold extraction since the introduction of the cyanide process (cyanide leaching, MacArthur and Robert Forrest, 1887), but of course, the investigation of the optimization and improvement of existing technologies and the development of new schemes to extract gold are continued.

The lack of high quality gold ores is one of the reasons for intensive research about possible pretreatment methods prior to leaching. As a consequence, the existing technological schemes of gold extraction become more complicated. Another reason is the environmental issues which forces to seek for more environmentally friendly alternatives.

Let us consider the major gold extraction process stages which are presented at the Figure 3.1.

Comminution of gold ores and concentrates is mainly required to liberate gold, from bearing minerals to make the mineral amenable to subsequent gold extraction steps (Marsden, et al., 2006). The necessary degree of comminution depends on various factors, such as the liberation size of gold, the size and nature of the host mineral particles, and the methods to be used for gold recovery. Besides the usual application of comminution for gold liberation prior flotation, gravity concentration, and leaching, it can be applied for refractory ore treatment, if needed (Marsden, et al., 2006), for liberation of sulfide minerals before flotation; optimization of particle size of sulfide mineral prior to oxidative pretreatment; ultrafine grinding of gold-bearing sulfide concentrate prior to leaching.

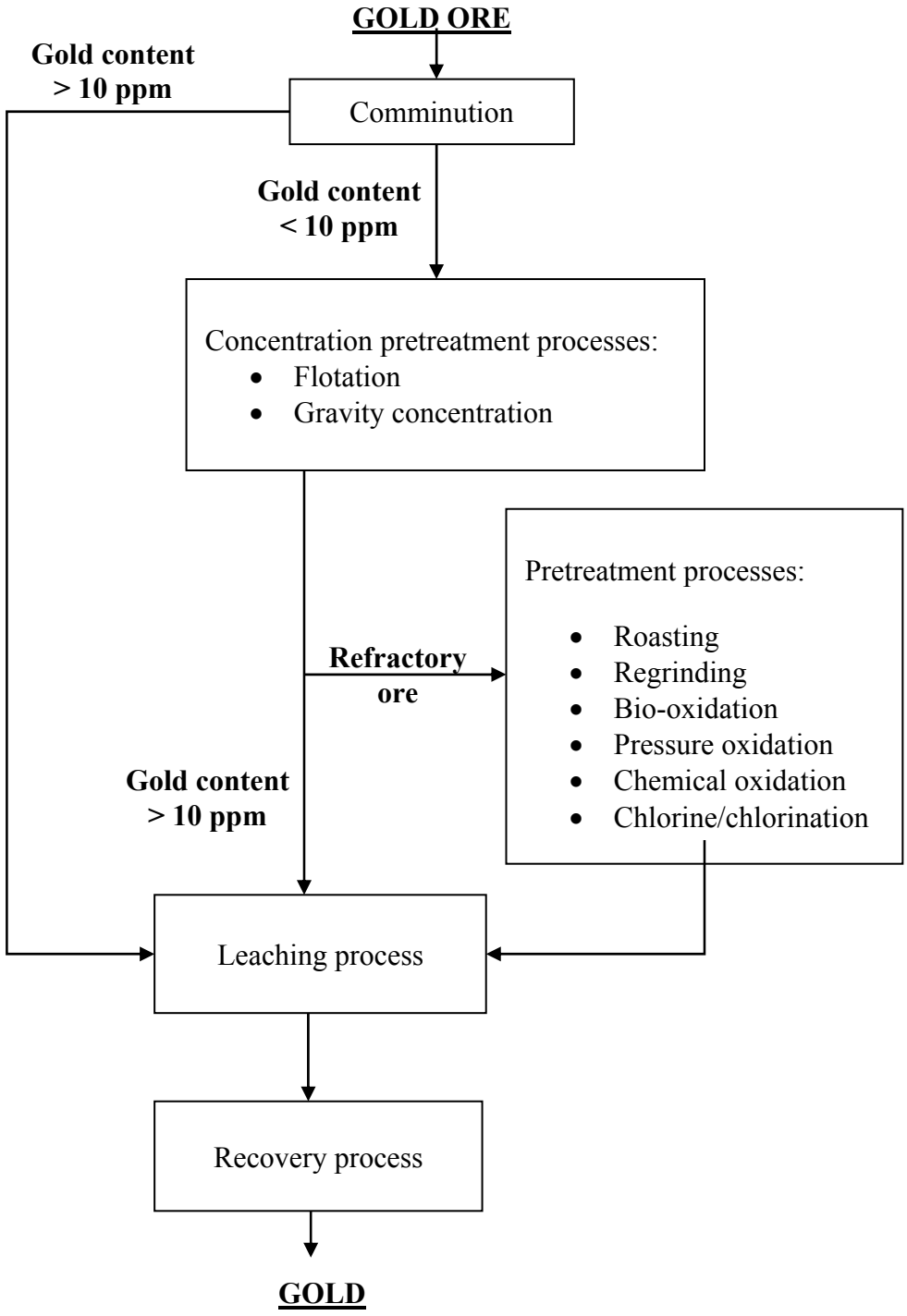

Figure 3.1 Basic flow diagram of gold recovery (Abrantes, et al., 2004; Elvers, et al., 1990).

Ore ***concentration*** is accomplished ahead of cyanidation in many gold extraction flow sheets, and is used to upgrade ores for the following reasons (Marsden, et al., 2006):

- to produce a high-grade gold concentrate in a small weight fraction;
- to reject a part of the ore which does not contain gold in order to decrease the bulk of feed to subsequent processes;
- to reject a barren part of the ore which would otherwise negatively effect on subsequent gold extraction, for example, cyanide-consuming sulfide minerals, gold-adsorbing carbonaceous minerals, and acid-consuming carbonate impurities.

Among the concentration methods, flotation and gravity concentration are widely used.

Gravity concentration can be applied for the recovery of free gold and gold associated with heavier minerals by using concentrating equipment such as jigs, shaking tables, spirals and centrifugal concentrations. The product of gravity concentration can be treated by direct cyanidation, amalgamation, floatation, or intensive cyanide leaching, depending on their mineralogy.

Flotation is one of the variants for processing gold ores which contain easily floatable minerals. The alternative ways to apply flotation are (Marsden, et al., 2006):

- flotation of free gold and gold-bearing sulfide minerals to obtain a gold-rich concentrate;
- flotation of gold sulfide minerals to obtain a sulfide-free slurry for subsequent cyanidation;
- flotation of carbonaceous material, carbonates, or other materials which have negative impact;
- differential flotation (for instance, separation of gold, gold-bearing pyrite, arsenopyrite, and pyrite).

Leaching is used in all hydrometallurgical gold extraction schemes in order to produce a gold-bearing solution as an intermediate product from which pure gold can be obtained by using different extraction processes (chemically or electrolytically). Leaching is a hydrometallurgical method for extracting a soluble constituent, such as gold or silver, from a solid by means of a solvent. Two objectives are expected to be achieved (Habashi, 1999):

- opening the structures of ores, concentrates or metallurgical products to solubilize the valuable components;
- leaching the easily soluble constituents of an ore or a concentrated in order to obtain a more concentrated or pure product.

Presently, dilute alkaline cyanide solution is applied exclusively for gold dissolution, although chlorine/chloride media have been used in the past (Marsden, et al., 2006). There are several potential alternatives to cyanide leaching which none yet has been used in large commercial scale: thiosulfate, thiocyanate, thiourea, iodide, and bromide solutions. As in any liquid-solid reactions, the rate of leaching depends on the following factors: particle size of solids, concentration of leaching agent, agitation, pulp density, and temperature. The properties of certain leaching agent such as cost, solubility of the material to be leached, selectivity, ability of regenerating, and corrosivity should be also taken into account. However, in some cases the variation of technological parameters cannot give acceptable result due to the initial resistance of solids for different leaching agents. In such cases the application of various pretreatment processes is a necessity.

The difficulties in refractory gold ores processing was considered above. To make them amenable to cyanidation, a sulfur oxidation process should be involved to expose the gold particles. Generally, the chemical reactivity of the majority of gold-bearing minerals significantly exceeds the chemical reactivity of gold. This fact leads to the possibility of selective dissolution or decomposition of these minerals while the liberated gold retain in the insoluble residue, from which the

gold could be easily extracted by cyanidation or other hydrometallurgical methods.

According to Figure 3.1, there exist various oxidative ***pretreatment processes***, which generally are divided to pyrometallurgical and hydrometallurgical methods:

- **Roasting** – the applying of roasting under oxidizing conditions is a very common pyrometallurgical process. The idea is to burn away the sulfur from dry ore by using heat and air. However, this process has been considered as a high energy consuming technology with environmental drawbacks such as the emission of gases the utilization of which require elaborate gas scrubbing systems that frequently produce sulfuric acid as a byproduct. (Carrillo-Pedroza, et al., 2012). Hence, the aqueous chemical oxidation methods have more attractive perspectives.
- **Regrinding** – the ultrafine grinding, as reported, results in a high degree of strain being introduced into the mineral lattice. Consequently, number of grain boundary fractures and lattice defects in the minerals increase by several orders of magnitude. This lowers the activation energy for the oxidation of the sulphides and facilitates leaching. The increased mineral surface area may also enhance the rate of leaching (Duncan, 2000).
- **Bio-oxidation** – the biological oxidation uses sulfur consuming bacteria (such as *Thiobacillus Ferrooxidans*) in water solution under optimal conditions (atmospheric pressure; low temperature 28-35^{0}C; pH 1,7-2,4; aeration by air). The rate of oxidation is relatively low and the retention time ranges from 15 to 150 hours with the level of sulfide mineral oxidation being 80-90% (Bhappu, 1990).
- **Pressure oxidation** – the essence of the method of pressure oxidation is the oxidation of sulfide gold concentrate in an aqueous medium under the action of oxygen at elevated temperatures. The oxidative pretreatment process is considered as one of the pretreatment

techniques for ores that give poor gold recoveries by conventional leaching or for which reagent consumption is prohibitively high. This process was considered more details in Chapter 4.

- **Chemical oxidation** – as examples of chemical oxidation two processes can be presented: atmospheric-pressure oxidation with nitric acid (Nitrox process) and catalytic oxidation technology using NOx. The first process is used to treat ore in nitric acid in the presence of air at atmospheric pressure. The second one is applied to treat ore using NOx oxidation in the presence of oxygen at atmospheric pressure. Both processes have the aim to oxidize pyrite and arsenopyrite prior to cyanidation.
- **Chlorine/chlorination** – chloridizing roasting is another attractive approach for processing sulfide minerals. In the chemical reactions during the chloridizing roast gold is converted into chloride and the sulfur is fixed as a sulfate (Mukherjee, et al., 1985).

A summary of the mentioned oxidative pretreatment processes is shown at the Table 3.2. Among the different pretreatment methods, the high-pressure oxidation of gold-sulphide established itself as a fairly simple and effective technique for extraction of dispersed gold in sulfides. Since 1985, the high-pressure oxidation method has been applied for more than 13 gold extraction plants. As compared with widely used roasting treatment method the autoclave technology has the following advantages (Naboichenko, et al., 2009):

- higher gold recovery can be achieved;
- absence of gas emissions of arsenic and sulfur;
- arsenic is obtained in the form of low-toxic ferric arsenate, which does not require special tailings storage;
- low sensitivity to the presence of impurities in the raw materials such as antimony and lead;
- the possibility of processing flotation concentrates and ores.

Table 3.2 Summary of oxidative pretreatment processes (Marsden, et al., 2006).

Process type	Oxidation method	State of development of technology	Ore types treated	Application examples
Hydrometallurgical	Low-pressure oxygen preaeration	Proven commercially	Mildly refractory which contain small quantities of reactive sulfides	East Driefontein (South Africa) Luipin (Canada) Lead (South Dakota, USA)
	High-pressure oxygen (acidic media)	Proven commercially	Refractory sulfidic and arsenical ores with low carbonates and high sulfur	McLaughlin (California, USA) Sao Bento (Brazil) Goldsrike, Lone Tree, Twin Creeks (Nevada, USA) Lihir and Porgera (Papua New Guinea) see more at the Table 4.1
	High-pressure oxygen (nonacidic media)	Proven commercially	Refractory sulfidic and arsenical ores with low carbonates and high sulfur	Mercur (Utah, USA)
	Nitric acid	Proven commercially for silver concentrates, unproven for gold	Refractory concentrates containing silver, copper, and antimony	Sunshine (Idaho, USA)
	Chlorine/chlorination	Proven commercially	Carbonaceous ores, low sulfur telluride ores	Carlin and Jerritt Canyon (Nevada) Emperor (Fiji)
	Biological	Proven commercially for flotation concentrates, unproven for whole-ore treatment	Refractory arsenical and sulfidic ores; gold preferably associated with arsenopyrite, marcasite	Fairview (South Africa) Sao Bento (Brazil) Wiluna and Youanmi (Australia) Ashanti Sansu (Ghana)
Pyrometallurgical	Roasting	Proven commercially	Refractory sulfidic, arsenical; carbonaceous and telluride ores	Campbell Red Lake and Giant Yelloknife (Canada) Kalgoorlie Consilidate-Gidli (Australia) New Consort (South Africa) Big Springs, Carlin, Cortez, and Jerritt Canyoun (Nevada)

High-pressure oxidation provides more complete oxidation of sulfides compared to biological method (including refractory pyrite) and therefore higher gold recovery can be achieved. The autoclave method is applicable both to ores and concentrates. Bioleaching, because of its low intensity and high volume of the required equipment, is only applicable to concentrates. In many cases, this can cause additional losses in gold enrichment.

Although the high-pressure process has relatively high capital and operational costs, it is capable of rapid oxidation of the majority of sulfidic and arsenical minerals in the feed. From an environmental point of view, the process is attractive due to production of very small amount of noxious gases (Marsden, et al., 2006).

4 HIGH PRESSURE PRETREATMENT PROCESS

4.1 High-pressure oxidation technology

Recently, processes occurring at high pressures and temperatures have acquired more and more importance in chemical engineering and hydrometallurgy of nonferrous metals. High-pressure processes, known as the autoclave processes, can be applied to gold-bearing raw materials in two ways:

- pressure oxidation of sulfides while the gold remains in the insoluble residue. After that, gold can be extracted from the residues by cyanidation or by using other hydrometallurgical methods;
- pressure leaching, which combines the oxidation of sulfides and the dissolution of gold into solution.

Consideration of the pressure leaching remains outside of the scope of this work, but the high-pressure oxidation process will be considered in more details. Although the oxidation of sulfide minerals can be done under acidic, alkaline and neutral conditions, the acidic media is applied more often in practice (see Chapter 1.1). Thus, the acidic high-pressure oxidation technology will be considered. This method is applicable for processing the flotation concentrates and ores.

A block diagrams of pyrite gold ore and concentrate processing is shown in Figure 4.1 and Figure 4.2 (Naboichenko, et al., 2009). Acidic pressure oxidation processes consist of three major steps:

- feed preparation;
- oxidation
- product neutralization

According Figure 4.1 the aim of the first stages, which include crushing, grinding, and thickening, is to obtain a pulp (where the particle size is generally 80-90% <74 μm). After that, acid treatment is applied in order to avoid the presence of carbonates in the pressure oxidation process.

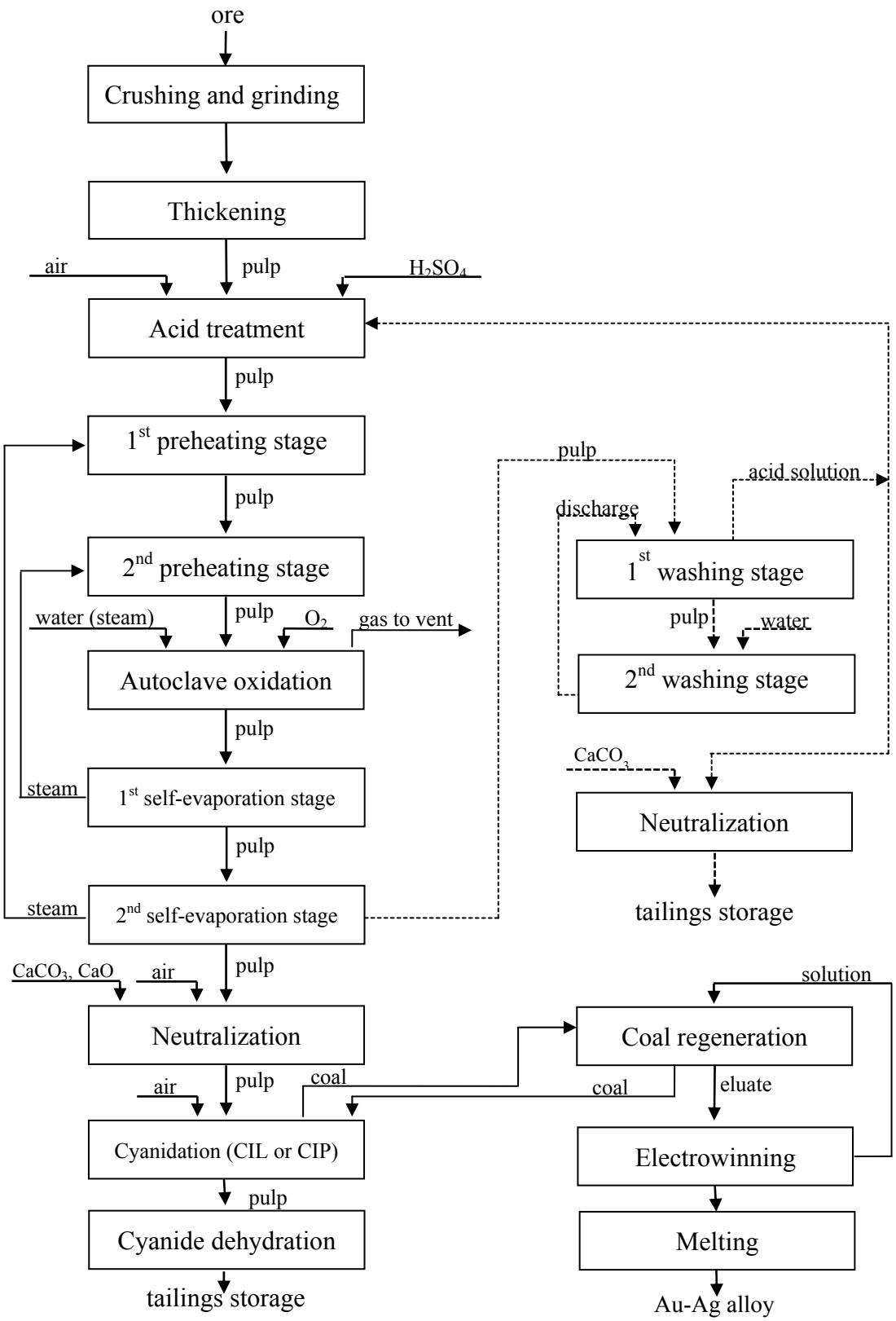

Figure 4.1 Block diagram of pressure oxidation of pyrite refractory gold ore (Naboichenko, et al., 2009).

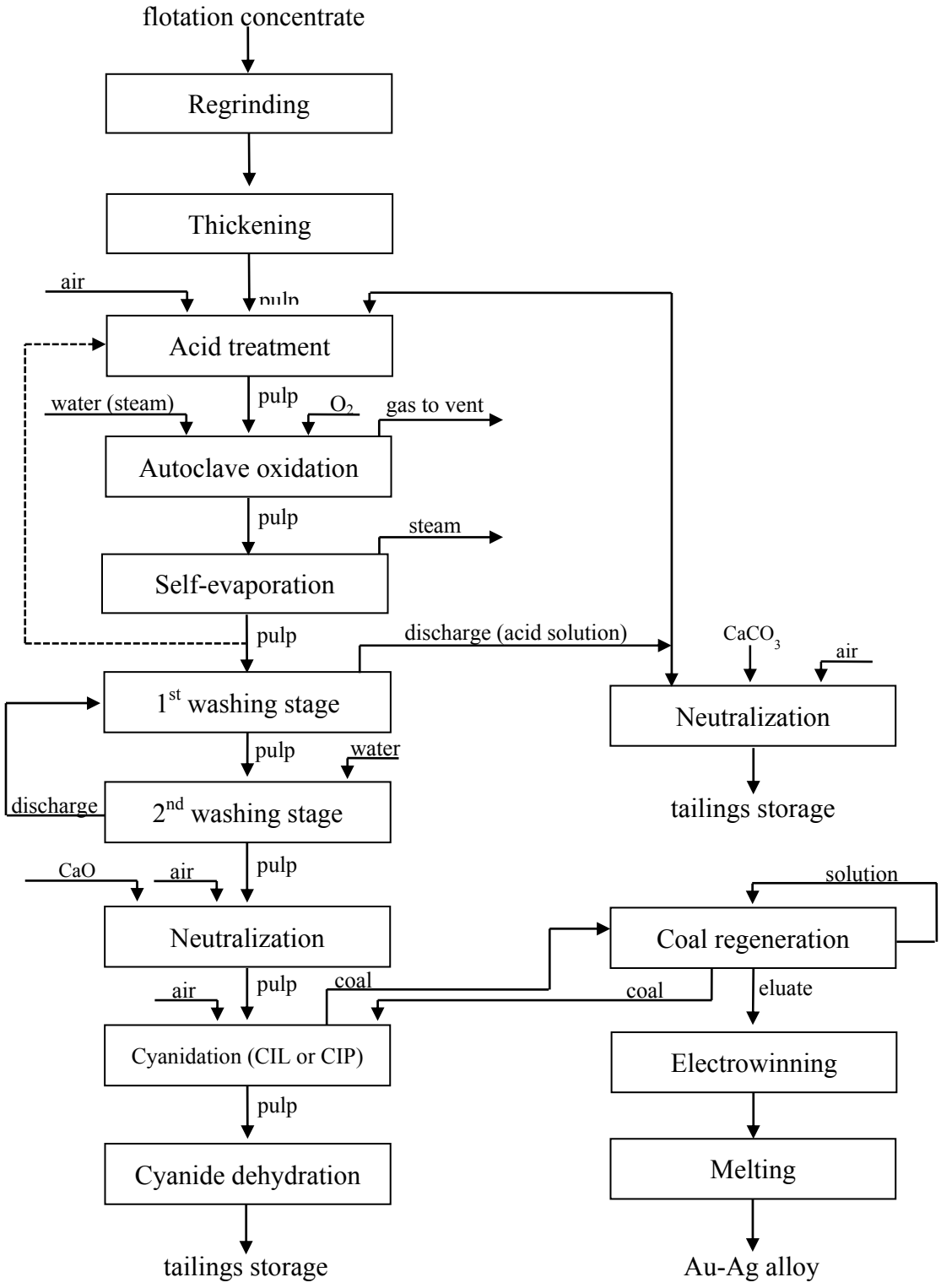

Figure 4.2 Block diagram of pressure oxidation of pyrite refractory gold concentrate (Naboichenko, et al., 2009).

The final pH of the slurry, which guarantees complete decomposition of carbonates, is maintained at 1.8-3.0 by addition of sulfuric acid or by recycling of an acidic solution. Antifoams such as lignosulfonates, can be used to avoid foaming of the pulp. The air is supplied to completely remove the carbon dioxide.

A sufficient level of sulphide content in the ore minerals allows operating the oxidation process autogenously. As a result of this, the process is performed utilizing the heat of exothermic reactions, thus steam is needed only at the start-up of the autoclave. Since the sulfide sulfur content in the ore usually does not exceeding 4-5%, which is insufficient to operate autogenously, the pulp is supplied to a set of preheaters (1 to 3).

After preheating stage, the pulp is ready for pressure oxidation by using horizontal multi-chambered autoclaves which are lined with acid-resistant bricks (see Chapter 4.2). The process is carried out at 450-500 K and the total pressure in the autoclave is in the range 1800-3200 kPa. The required duration of the pressure oxidation is usually not more than 1-1.5 hours (Naboichenko, et al., 2009).

The oxidized pulp as a product of the autoclave oxidation is cooled and supplied to neutralization with lime milk. The raise of pH to 10-10.5 leads to formation of gypsum and iron hydroxide. Arsenic is deposited as an amorphous ferric arsenate in variable composition $FeAsO_4 \cdot Fe(OH)_3$. In some cases, during the neutralization of the pulp a significant increase in its viscosity occurs due to formation of large amounts of sludge of hydroxides and arsenates of iron, aluminum, magnesium and other metals. This leads to deteriorating conditions of mass transfer during cyanidation. To overcome this problem the pulp is washed before neutralization by countercurrent decantation in a system of two or three thickeners. The separation of the acidic liquid phase make it possible to avoid the mentioned difficulties (Naboichenko, et al., 2009).

The washed slurry after neutralization is delivered to cyanidation. As sorbent ion-exchange resins and activated carbon may be used. The last one has more wide application and can be implemented in two ways: CIP (Carbon in Pulp) and CIL

(Carbon in Leach). The CIP process is applied to treat ores containing finely divided clay particles which are difficult to filter. The CIP process involves the agitation of cyanide leaching pulp in tanks with adsorbent pellets. When adsorption is finished, the pulp is screened to separate the gold-laden pellets for washing and desorption. The CIL process is applied to treat ores containing organic matter. Since organic matter can behave as an adsorbent, the presence of organic matter renders the gold cyanide complex susceptible to being lost as residue. The use of the CIL process requires that the granular activated carbon which is added in the leaching tanks, adsorbs the gold cyanide complex during its formation and more effectively than the organic matter. The charged carbon is separated from the pulp by screening (Habashi, 1999). The tails after cyanidation which contain arsenic in the form of poorly soluble and relatively non-toxic scorodite is sent to the tailings pond.

The charged carbon is regenerated. Thus, a concentrated gold solution is obtained. The recovery of gold metal from the concentrated gold solution, with or without an intermediate concentration and purification stages, is performed by reduction process, such as zinc precipitation or cementation and electrowinning (Marsden, et al., 2006).

A flow sheet of pressure oxidation of pyrite refractory gold concentrate is shown in Figure 4.2. Due to high content of sulfur in the concentrate, the stages of regeneration of heat are not needed. This is the main difference compared to Figure 4.1. Since the concentrate, which is obtained from the leaching solution, has a high concentration of sulfuric acid and iron, the neutralization of such concentrate is impossible. For that reason, the scheme uses countercurrent washing of the pulp by thickeners. Acidic solutions are fed to neutralization and partially to acid treatment. In some cases, part of the leached pulp after self-evaporation is supplied to the acid treatment that allows to use the acid contained in the pulp and to reduce the sulfur content in the feed of the autoclave. That facilitates to operate the process autogenously and to reduce the risk of formation of elemental sulfur and the related complications (Naboichenko, et al., 2009).

4.2 Application of autoclave for high-pressure oxidation process

The autoclaves are versatile reactors for used in high-pressure hydrometallurgical processes. A typical autoclave consists of multiple compartments. The ore or concentrate is fed to the reactor as slurry which is preheated by vapor. The required preheat temperature is determined by the calorimetric value of the feed. Since the oxidation process of sulfides is exothermic it can be observed that the heat produced by oxidation is proportional to the arsenic and sulphide content in the feed (Baldwin, et al., 1998). The quantity of heat which is generated by the oxidation reaction of pyrite and arsenopyrite is 12000 and 8500 kJ per 1 kg of sulfide, respectively (Naboichenko, et al., 2009). Thereby, the weight content of sulphide and arsenic in the feed represents the fuel content and the conditions for the pressure oxidation process can be varied by recycling oxidized solids, as displayed in Figure 4.3.

If the sulfur content is high (more that 6%) removal of extensive heat is required. The application of embedded heat exchangers for that purpose is inefficient due to mineral depositions and subsequent reduction in heat transfer coefficient. Controlling the temperature by discharging exhaust gases leads to a decrease in the degree of oxygen utilization. Most often, heat is removed by adding cold aqueous feed into each compartment of the autoclave. In the first compartment, which is fed by cold pulp, there might be lack of heat and steam is needed. For minimization of steam consumption in the first compartment, the first compartment is often made large compared to the size of the other compartments. This can be achieved by removing the partition wall between the first and second (and sometimes the third) compartments. Controlling the excess heat by supplying water into the autoclave is also justified due to the absence of valuable components in the liquid phase. Thus, dilution by water does not cause complications in subsequent operations. Furthermore, the dilution of the pulp reduces its viscosity and facilitates further separation of solid and liquid phases (Naboichenko, et al., 2009).

Low sulfur content (less than 6%) requires that the feed is preheated prior to autoclave oxidation.

The autoclave operates under high total pressure. Therefore, the solubility of oxygen, which is sparged into each compartment, is sufficient for efficient rate of reactions. The discharge from the autoclave contains: metal ion solution, which is sent to refinery; and oxidized solids, which include the precious metals and are subjected to several stages of cooling and neutralization before cyanidation (Baldwin, et al., 1998).

The autoclaves usually have a shape of cylinders vertically mounted or horizontally laid. Agitation in an autoclave can be performed by injecting high-pressure steam, mechanically or by rotating the whole autoclave. Industrial autoclaves have volumes of 10 to 70 m^3 and operate at 2500-5000 kPa (Habashi, 1999). Figure 4.4 shows a schematic of a horizontal autoclave with mechanical agitation by impellers. This type of equipment is commonly used for the oxidation of pyrite and arsenopyrite to liberate gold prior to cyanidation.

Some plants which apply autoclaves for treatment of gold ores and concentrates are listed at the Table 4.1. Since 1985, the autoclave pretreatment method has been applied by more than 12 companies. In these factories flotation concentrates and ores have been successfully treated. The characteristic of the feed stock is highly varied not only in gold content, but also in chemical and mineralogical composition. Generally, horizontal large volume multi-chambered autoclaves with agitators are often used for oxidation.

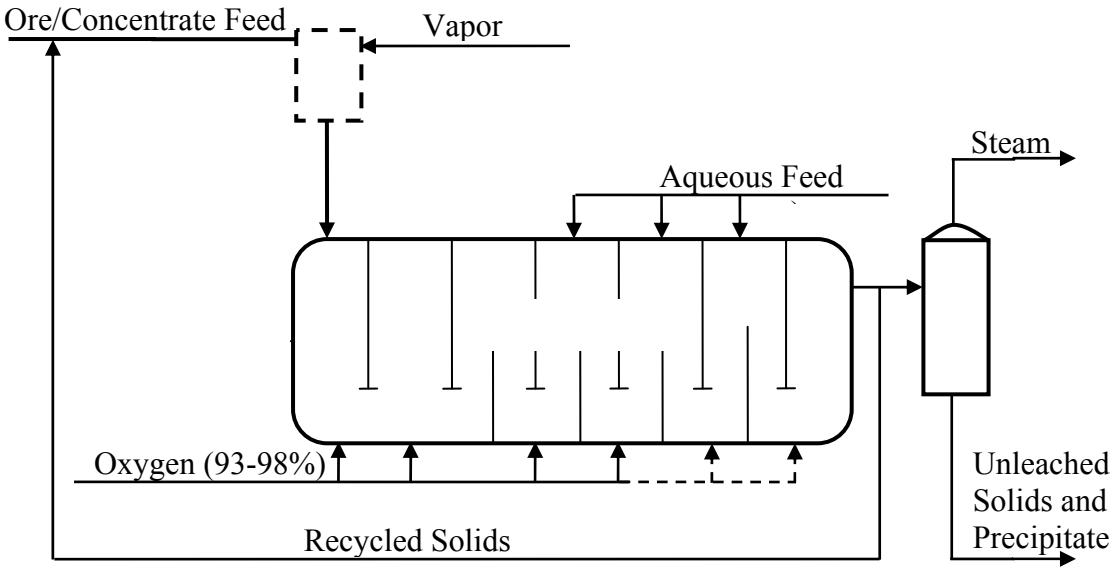

Figure 4.3 Flow diagram of autoclave gold oxidation process (Baldwin, et al., 1998).

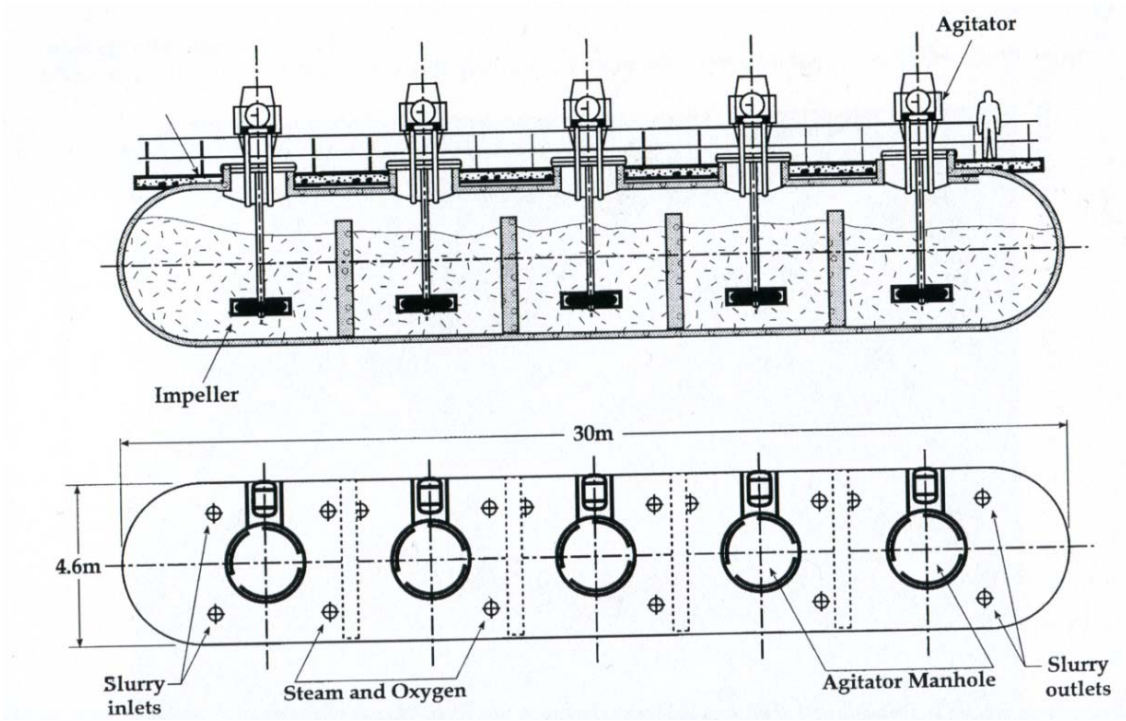

Figure 4.4 A large industrial autoclave 4,6 m diameter and 30 m long, lined with acid-resisting bricks, used for the oxidation of pyrite and arsenopyrite to liberate gold prior to cyanidation (Habashi, 1999).

Table 4.1 Plants which apply autoclave method for refractory gold ores and concentrates (Naboichenko, et al., 2009; Habashi, 1999).

Startup	The plant location	Owner	Feed	Medium	Capacity, tons/day	Feed Size	Parameters of Oxidation Autoclave							Oxidation level Ss, %
							Num.	Enclosed volume, m^3	Dimensions diam.×len., m	Num. of comp.	Temp., ^0C	Press., kPa	Res. time, min	
1985	McLaughlin, USA	Homestake, USA	ore	acid	3000	80% 75 μm	3	130	4,2 x 16	4	180	2200	60	85
1986	San Bento, Brazil	Genmin, South Africa	conc.	acid	240	90% 44 μm	2	[no data]	3,5 x 21	5	190-200	1600	120	95
1988	Mercur, USA	American Barrick, Canada	ore	alkaline	700	80% 75 μm	1	[no data]	3,7 x 13,3	4	215	3200	90	70
1989	Getchell, USA	First Miss Gold	ore	acid	2700	80% 75 μm	3	165	3 x 30	5	210	3100	90	95
1990	Goldstrike, Nevada, USA	American Barrick, Canada	ore	acid	16000	80% 135 μm	6	230	3,9 x 20,4	5	215-220	2900	50	90-92
1991	Porgera, P.-N. Guinea	Placer Dome, Canada	conc.	acid	2100	80% 37 μm	4	160	3,57 x 27	5	190-200	1800	110	99
1991	Cambell, Canada	Placer Dome, Canada	conc.	acid	100	80% 73 μm	1	[no data]	2,8 x 15,2	5	200	2100	120	99
1994	Lone Tree, USA	[no data]	ore	acid	2300	80% 75 μm	1	170	3,9 x 19,3	4	196	1860	50	55-75
1997	Lihir, Papua N. Guinea	[no data]	ore	acid	11400	80% 106 μm	3	[no data]	4,5 x 31,2	6	205	2650	65	98
1997	Twin Creeks, USA	[no data]	ore	acid	7200	80% 22 μm	2	340	6 x 23,1	4	225	3200	50	97
1999	Macraes, N. Zealand	[no data]	conc.	acid	560	80% 18 μm	1	57	3,5 x 12,6	3	225	3140	45	92-98
1999	Hillgrove, Australia	[no data]	conc.	acid	24	[no data]	1	[no data]	2,2 x 8,4	5	220	3180	145	[no data]

5 MODELING OF HIGH PRESSURE OXIDATION PROCESS

5.1 Assumptions and model approximations

In this works a mathematical model is developed to describe oxidation kinetics in batch scale laboratory experiments. The developed high pressure oxidation process model includes several assumptions:

- the model is pseudo-homogeneous and do not take into account the effects of particle size distribution and population balances of the concentrate particles;
- the solids are treated as a pseudo-homogeneous phase and local average particle size is calculated from the pyrite conversion. The mixing in laboratory experiments is intensive. Therefore, the reaction of pyrite oxidation is chemically controlled. Thus, based on the shrinking core model, the shrinkage of the particle core can be described by the following equation:

$$\left(\frac{d_i}{d_o}\right)^3 = 1 - x_{FeS_2} \qquad (7)$$

where d_i - inner diameter of particle, m

d_o - outer diameter of particle, m

x_{FeS_2} - pyrite conversion

- the reaction rate of pyrite is specified as a surface reaction (mol FeS_2 /m^2 min) between oxygen - pyrite and ferric ions - pyrite. Thus, reactions between pyrite, dissolved oxygen and ferric ions take place at the reactive surface of the particle according to Equation (R29) and

(R30). The active area, therefore, continuously decreases as the reactions proceed;

- the kinetics of the surface reaction depends on the concentration of pyrite (in the solids), ferric ions, dissolved oxygen, and pyrite conversion;
- the passivation of the mineral surface, most likely by elemental sulfur, can effect on pyrite conversion. Term $(1-x_{FeS_2})^{n_i}$ takes into account the possibly occurring negative effects on pyrite oxidation rate as the reaction proceeds. It is assumed that passivation have different influence on pyrite oxidation by oxygen and by ferric ions.
- pyrite concentration at the solid surface of the particle is characteristic for the concentrate and can be assumed to remain constant during oxidation;
- the reaction where ferrous ions is oxidized back to ferric iron is a bulk reaction;
- the dependency of the surface reaction rate and the bulk reaction rate on temperature is taken into account by the Arrhenius equation.

5.2 High pressure oxidation process model

High pressure oxidation process can be represented by using the following mass transfer phenomena and chemical reactions:

- oxygen mass transfer:

$$O_{2(g)} \rightarrow O_{2(aq)} \qquad \text{(R37)}$$

- pyrite oxidation by dissolved oxygen (solid/liquid reaction):

$$FeS_{2(s)} + 7/2O_{2(aq)} + H_2O \xrightarrow{r_1} FeSO_{4(aq)} + H_2SO_{4(aq\ )} \qquad \text{(R38)}$$

- pyrite oxidation by Fe^{3+} (solid/liquid reaction):

$$FeS_{2(s)} + 7Fe_2(SO_4)_{3(aq)} + 8H_2O \xrightarrow{r_2} 15FeSO_{4(aq)} + 8H_2SO_{4(aq)} \quad \text{(R39)}$$

- Fe^{2+}/Fe^{3+} oxidation in liquid phase (homogeneous reaction):

$$2FeSO_{4(aq)} + 1/2O_2 + H_2SO_{4(aq)} \xrightarrow{r_3} Fe_2(SO_4)_{3(aq)} + H_2O \quad \text{(R40)}$$

Kinetic equations of oxidation process:

- the oxygen mass balance:

$$\frac{dc_{L,O_2}}{dt} = k_L a(c^*_{L,O_2} - c_{L,O_2}) - 7/2 r_1 A_i n\varepsilon - 1/4 r_3 \, [mol/L_{liq} \min] \quad (8)$$

where $k_L a$ - the mass transfer coefficient times the specific surface area of the oxygen bubbles, 1/min

c_{L,O_2} - dissolved oxygen concentration in liquid phase, mol/L

c^*_{L,O_2} - dissolved oxygen concentration at saturation point in liquid phase, mol/L

r_1 - surface reaction rate between pyrite and oxygen, mol m^2/min

r_3 - reaction rate between pyrite and ferric ions, mol L/min

A_i - inner surface area of particle (reactive area), m^2

n - number of solid particles in reactor per liter slurry, 1/L

ε - volume fraction of liquid in the slurry.

The dependence of the molar saturation concentration of dissolved oxygen on the oxygen partial pressure is evaluated by the Tromans (1998) model:

$$c^*_{L,O_2} = 101325\psi \exp\left(\frac{-0.046T^2 + 203.35T\ln T - 1430.55T + 68669}{8.3143T}\right) P_{O_2}\ [mol/L_{liq}] \quad (9)$$

$$\psi = \left(\frac{1}{1 + 2.01628\,[H_2SO_4]}\right)^{0.168954} \quad (10)$$

where c^*_{L,O_2} - dissolved oxygen concentration at saturation point in liquid phase, mol/L

T - temperature, K

$[H_2SO_4]$ - molal concentration of H_2SO_4, mol/kg H_2O

P_{O_2} - partial pressure of oxygen in the gas phase, Pa

- the surface reaction of pyrite with oxygen and Fe^{3+}:

$$\frac{dx_{FeS_2}}{dt} = \frac{(r_1 + r_2)A_i n}{c_{FeS_2,0}}[1/\min] \quad (11)$$

where r_1 - surface reaction rate between pyrite and oxygen, mol m^2/min

r_2 - surface reaction rate between pyrite and ferric ions, mol m^2/min

A_i - inner surface area of one particle (reactive area), m^2

n - number of solid particles in reactor per liter slurry, 1/L

$c_{FeS_2,0}$ - initial pyrite concentration per liter of slurry, mol/L

Based on the shrinking core model, the inner surface area of the particle can be described by the following equation:

$$A_i = \pi(1 - x_{FeS_2})^{2/3} d_0^2 \, [m^2] \qquad (12)$$

where x_{FeS_2} - pyrite conversion

d_0 - outer diameter of particle, m

The number of solid particles in reactor per liter slurry is calculated by using the mean particle size:

$$n = \frac{V_{FeS_2}}{\frac{\pi}{6} d_{mean}^3 V_{slurry}} [1 / L_{slurry}] \qquad (13)$$

where V_{FeS_2} - volume of pyrite, m^3

V_{slurry} - volume of slurry, L

d_{mean} - mean particle size, m

The mean particle size was taken as the square root of the product of two adjacent sieve sizes.

- production of Fe^{3+}:

$$\frac{dc_{Fe^{3+}}}{dt} = -7r_2 A_i n\varepsilon + 1/2r_3 \, [mol / L_{liq} \, \min] \qquad (14)$$

where $c_{Fe^{3+}}$ - concentration of ferric ions per liter liquid phase, mol/L

r_3 - reaction rate between ferrous iron and oxygen, mol L/min

- production of Fe^{2+}:

$$\frac{dc_{Fe^{2+}}}{dt} = r_1 A_i n\varepsilon + 15 r_2 A_i n\varepsilon - r_3 [mol / L_{liq} \text{ min}] \qquad (15)$$

where $c_{Fe^{2+}}$ - concentration of ferrous ions per liter liquid phase, mol/L

The reaction rates are represented as:

- the surface reaction rate between pyrite and oxygen:

$$r_1 = k_1 c_{FeS_2,0} (1 - x_{FeS_2})^{n_1} c_{L,O_2}^{n_2} [mol / m^2 \text{ min}] \qquad (16)$$

$$k_1 = k_{1,mean} \exp\left(-\frac{E_1}{R} \left(\frac{1}{T} - \frac{1}{T_{mean}} \right) \right) \qquad (17)$$

where n_1 - reaction order for pyrite conversion

n_2 - reaction order for concentration of dissolved oxygen

k_1 - reaction rate constant

$k_{1,mean}$ - reaction rate constant at mean temperature

E_1 - activation energy, kJ/mol

T_{mean}- mean temperature, K

R - gas constant, R=0.008314 kJ/mol K

- the surface rate constant of reaction of pyrite with Fe^{3+}:

$$r_2 = k_2 c_{FeS_2,0} (1 - x_{FeS_2})^{n_3} c_{Fe^{3+}}^{n_4} [mol / m^2 \text{ min}] \qquad (18)$$

$$k_2 = k_{2,mean} \exp\left(-\frac{E_2}{R} \left(\frac{1}{T} - \frac{1}{T_{mean}} \right) \right) \qquad (19)$$

where: n_3 - reaction order for pyrite conversion

n_4 - reaction order for concentration of ferric ions

k_2 - reaction rate constant

$k_{2,mean}$ - reaction rate constant at mean temperature

E_2 - activation energy, kJ/mol

- the bulk reaction rate of Fe^{2+} with oxygen to produce Fe^{3+}:

$$r_3 = k_3 c_{Fe^{2+}}^2 c_{L,O_2} \; [mol / L_{liq} \; \text{min}] \tag{20}$$

$$k_3 = k_{3,mean} \exp\left(-\frac{E_3}{R}\left(\frac{1}{T} - \frac{1}{T_{mean}} \right) \right) \tag{21}$$

where: k_3 - reaction rate constant

$k_{3,mean}$ - reaction rate constant at mean temperature

E_3 - activation energy, kJ/mol

Unknown model parameters are:

- E_1 activation energy, kJ/mol
- E_2 activation energy, kJ/mol
- E_3 activation energy, kJ/mol
- $k_{1,mean}$ reaction rate constant at mean temperature
- $k_{2,mean}$ reaction rate constant at mean temperature
- $k_{3,mean}$ reaction rate constant at mean temperature
- $k_L a$ volumetric mass transfer coefficient, 1/min
- n_1 reaction order for pyrite conversion

- n_2 reaction order for concentration of dissolved oxygen
- n_3 reaction order for pyrite conversion
- n_4 reaction order for concentration of ferric ions

5.3 Estimation of model parameters

5.3.1 Available experimental data

As the starting point of model parameters estimation, the experimental data presented by Long and Dixon (2003) was used for kinetic model development. In their study high-grade massive pyrite specimens originated from Zacateces (Mexico) was used as a raw material during experiments. The conditions of pressure oxidation experiments are shown in Table 5.1. The experimental conditions are presented in Table 5.2. Thus, the effects of temperature (170-230 ^{0}C), particle size (49-125 μm diameter), oxygen partinal pressure (345-1035 kPa), and pulp density (1-20 g/L) were evaluated in order to investigate pyrite oxidation kinetics. The catalytic effect of Cu(II) was also observed. For each test the experimental results were collected. These results inlude pyrite conversion, changes in particle size, and ratio between Fe^{3+} and Fe_{total}. Finally, tests from 1 to 9 were chosen for parameters estimation.

Table 5.1 Conditions of pressure oxidation experiments (Long, et al., 2004).

Parameter	Value
Agitation speeds, rpm	650-950
Temperatures, ^{0}C	170-230
Mean particle size, μm	49-125
Oxygen partial pressure, kPa	345-1035
Pyrite pulp desities, g/L	1-20
Acid concentration [H_2SO_4], M	0.5
Purity of the pyrite samples, %	97±1
Mole ratio of sulfur to iron	1.92
Reactor	2-L Parr titanium autoclave with maintaining a desired temperature and rate of stirring.

Table 5.2 Experimental plan (Long, et al., 2004).

Test. no	T, ^{0}C	d_0, µm	Agitation, rpm	P_{O2}, kPa	[FeS_2], g/L	[$CuSO_4$], g/L	[H_2SO_4], M	τ, min
The effect of temperature								
1	230	-74 + 53	800	690	1	0	0.5	25.6
2*	210	-74 + 53	800	690	1	0	0.5	38.7
3	190	-74 + 53	800	690	1	0	0.5	59.9
4	170	-74 + 53	800	690	1	0	0.5	99.1
The effect of particle size								
2*	210	-74 + 53	800	690	1	0	0.5	38.7
5	210	-149 + 105	800	690	1	0	0.5	77.3
6	210	-105 + 74	800	690	1	0	0.5	53.3
7	210	-53 + 44	800	690	1	0	0.5	28.7
The effect of oxygen partial pressure								
2*	210	-74 + 53	800	690	1	0	0.5	38.7
8	210	-74 + 53	800	1035	1	0	0.5	31.5
9	210	-74 + 53	800	345	1	0	0.5	52.9
The effect of pyrite pulp density and the addition of copper								
2*	210	-74 + 53	800	690	1	0	0.5	38.7
10	210	-74 + 53	800	690	20	0	0.5	25.4
11	210	-74 + 53	800	690	1	5	0.5	32.0
12	210	-74 + 53	800	690	20	5	0.5	16.9

* Standard conditions; τ – time required for complete reaction, min

The effects of pyrite pulp density and the addition of copper were not taken into account. All the results of the experiments, which were used for parameters estimation are represented in Appendix I.

The kinetics and the rate-controlling steps of a fluid-solid reaction are determined by noting how the progressive conversion of particles is influenced by particle size and operating temperature. Figure 5.1 shows the progressive conversion of spherical solids when chemical reaction, film diffusion, and ash diffusion are rate controlling steps. Figure 5.2 indicates the results of kinetic runs provided by Long and Dixon (2003). Comparing these two figures the rate controlling step can be predicted. At the beginning of the reaction, chemical reaction control is the most probable for our case. But, the difference between ash diffusion and chemical reaction as controlling steps is not significant and can be masked by the scatter in the experimental data.

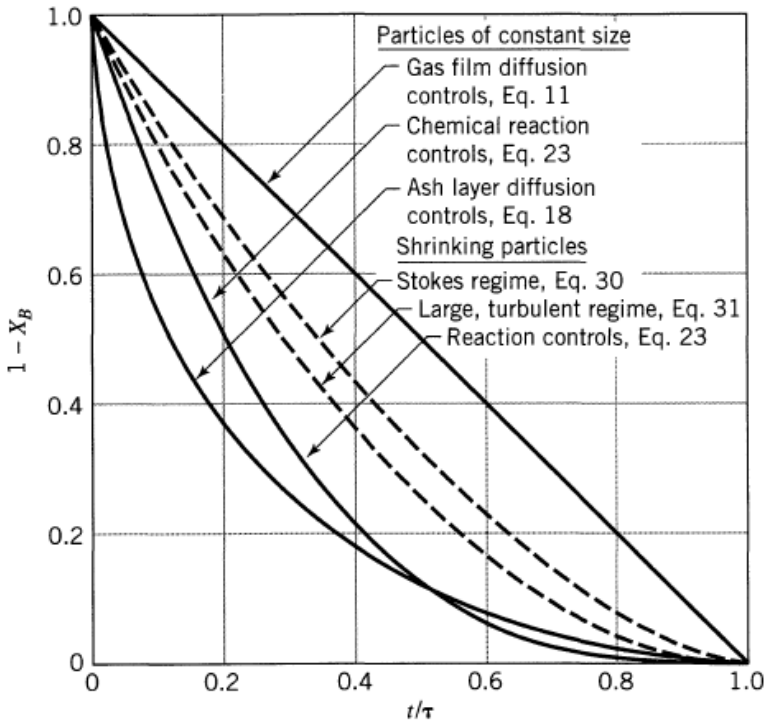

Figure 5.1 Progress of reaction of a single spherical particle with surrounding fluid measured in terms of time for complete conversion (Levenspiel, 1999).

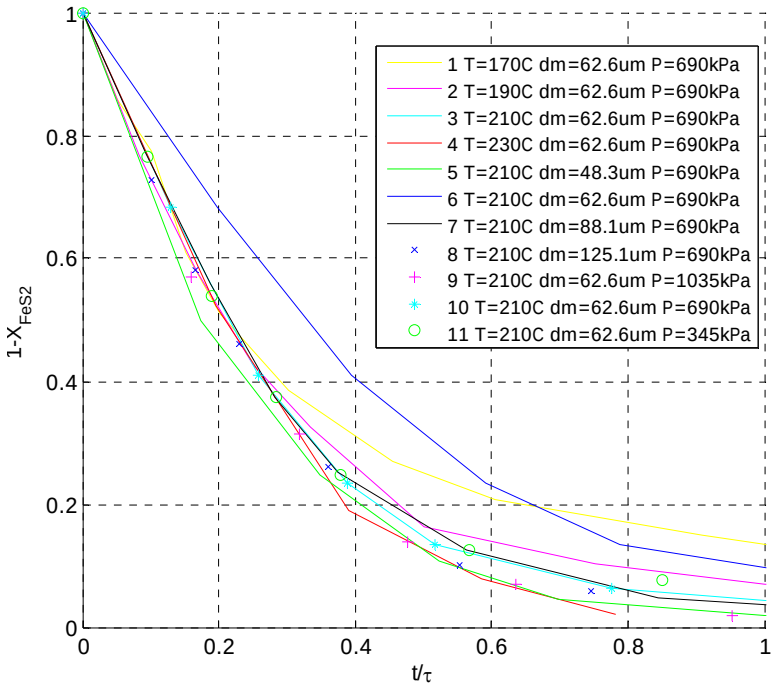

Figure 5.2 Progress of reaction of a single spherical particle with surrounding fluid measured in terms of time for complete conversion (experimental data by Long, et al., 2003).

5.3.2 Parameter estimation

During the procedure of parameter estimation several versions of model are suggested. All these models based on the above mentioned assumptions, reaction rates and differential equations. But, there are several assumptions which explain the difference between the various versions of the oxidation model:

- 1st model include all eleven parameters and the full set of differential equations. The passivation effect has separate impact on pyrite oxidation by oxygen (n_1) and ferric ions (n_3).

- 2nd model include ten parameters and the full set of differential equations. The passivation effect has equal impact on pyrite oxidation by oxygen and ferric ions.

- 3rd model include ten parameters and the full set of differential equations. The passivation effect has separate impact on pyrite oxidation by oxygen (n_1) and ferric ions (n_3). Concentration of dissolved oxygen remains constant during the experiments and equals the saturation concentration of saturation.

- 4th model include nine parameters and the full set of differential equations. The passivation effect has separate impact on pyrite oxidation by oxygen (n_1) and ferric ions (n_3). The concentration of dissolved oxygen remains constant during the experiments and equals the saturation concentration. The half-order reaction rate of pyrite dissolution by oxygen is assumed as the most probable rate eqution.

- 5th model include nine parameters and the full set of differential equations. The passivation effect has equal impact on pyrite oxidation by oxygen and ferric ions. The concentration of dissolved oxygen remains constant during the experiments and equals the saturation concentration. The half-order reaction rate of pyrite dissolution by oxygen is assumed as the most probable rate eqution

Table 5.4 and Table 5.5 represent model frameworks for each model and the values of the estimated parameters. The MATLAB toolbox Simulink Parameter

Estimation 1.2.2 was used for the estimation of the unknown parameters. Options of the estimation are shown in Table 5.3.

Table 5.3. Options of parameters estimation.

ODE Solver	ode45 (Domand-Prince)
Optimization method	Nonlinear least squares
Cost function	SSE (Error Sum of Squares): $SSE = \sum (y_i - \bar{y})^2$
Input parameters	Oxygen partial pressure Temperature Particle mean size
Output parameters	Pyrite conversion

For each model the goodness of fit was determined by using the R^2 value:

$$R^2 = 1 - \frac{\sum (y_i - f(x_i, b))^2}{\sum (y_i - \bar{y})^2} \qquad (22)$$

and the standard error:

$$STDErr = \sqrt{\frac{\sum (y_i - f(x_i, b))^2}{N - n}} \qquad (23)$$

where: y_i - values of experimental data

$f(x_i, b)$ - model prediction

N - number of samples

n - number of model parameters

The reliability of the models and their parameters is investigated by using the so-called Markov Chain Monte Carlo (MCMC) methods. The MCMC method are based on Bayesian inference and give a distribution of solutions. The MCMC methods have recently been successfully applied in chemical engineering to study parameter reliability. This method is also implemented in a MATLAB package (Haario, et al., 2006).

Table 5.4. Model frameworks.

<table>
<tr><th>Model №</th><th>Model framework</th><th>Result of estimation</th></tr>
<tr><td>1</td><td>$\frac{dc_{L,O_2}}{dt} = k_L a(c^*_{L,O_2} - c_{L,O_2}) - 7/2 r_1 A_i n\varepsilon - 1/4 r_3 \quad \frac{dx_{FeS_2}}{dt} = \frac{(r_1 + r_2) A_i n}{c_{FeS_2,0}}$
$\frac{dc_{Fe^{3+}}}{dt} = -7 r_2 A_i n\varepsilon + 1/2 r_3 \quad \frac{dc_{Fe^{2+}}}{dt} = r_1 A_i n\varepsilon + 15 r_2 A_i n\varepsilon - r_3$
$r_1 = k_1 (1 - x_{FeS_2})^{n_1} c^{n_2}_{L,O_2}$ where $k_1 = k_{1,mean} \exp\left(-E_1/R\left(1/T - 1/T_{mean}\right)\right)$
$r_2 = k_2 (1 - x_{FeS_2})^{n_3} c^{n_4}_{Fe^{3+}}$ where $k_2 = k_{2,mean} \exp\left(-E_2/R\left(1/T - 1/T_{mean}\right)\right)$
$r_3 = k_3 c^2_{Fe^{2+}} c_{L,O_2}$ where $k_3 = k_{3,mean} \exp\left(-E_3/R\left(1/T - 1/T_{mean}\right)\right)$</td><td>
<table>
<tr><th colspan="4">Estimated Parameters</th></tr>
<tr><th>Parameter</th><th>Value</th><th>Parameter</th><th>Value</th></tr>
<tr><td>E_1, kJ</td><td>29.251</td><td>k_La</td><td>166.53</td></tr>
<tr><td>E_2, kJ</td><td>71.716</td><td>n_1</td><td>2.41</td></tr>
<tr><td>E_3, kJ</td><td>10.001</td><td>n_2</td><td>0.69</td></tr>
<tr><td>$k_{1,\ mean}$</td><td>1.000e5</td><td>n_3</td><td>1.27</td></tr>
<tr><td>$k_{2,mean}$</td><td>7.959e6</td><td>n_4</td><td>2.00</td></tr>
<tr><td>$k_{3,mean}$</td><td>2.859e5</td><td></td><td></td></tr>
<tr><th colspan="4">Goodness of fit</th></tr>
<tr><td colspan="3">R^2</td><td>0.9943</td></tr>
<tr><td colspan="3">Std Err</td><td>0.0266</td></tr>
</table>
</td></tr>
<tr><td>2</td><td>$\frac{dc_{L,O_2}}{dt} = k_L a(c^*_{L,O_2} - c_{L,O_2}) - 7/2 r_1 A_i n\varepsilon - 1/4 r_3 \quad \frac{dx_{FeS_2}}{dt} = \frac{(r_1 + r_2) A_i n}{c_{FeS_2,0}}$
$\frac{dc_{Fe^{3+}}}{dt} = -7 r_2 A_i n\varepsilon + 1/2 r_3 \quad \frac{dc_{Fe^{2+}}}{dt} = r_1 A_i n\varepsilon + 15 r_2 A_i n\varepsilon - r_3$
$r_1 = k_1 (1 - x_{FeS_2})^{n_1} c^{n_2}_{L,O_2}$ where $k_1 = k_{1,mean} \exp\left(-E_1/R\left(1/T - 1/T_{mean}\right)\right)$
$r_2 = k_2 (1 - x_{FeS_2})^{n_1} c^{n_3}_{Fe^{3+}}$ where $k_2 = k_{2,mean} \exp\left(-E_2/R\left(1/T - 1/T_{mean}\right)\right)$
$r_3 = k_3 c^2_{Fe^{2+}} c_{L,O_2}$ where $k_3 = k_{3,mean} \exp\left(-E_3/R\left(1/T - 1/T_{mean}\right)\right)$</td><td>
<table>
<tr><th colspan="4">Estimated Parameters</th></tr>
<tr><th>Parameter</th><th>Value</th><th>Parameter</th><th>Value</th></tr>
<tr><td>E_1, kJ</td><td>98.961</td><td>k_La</td><td>34.73</td></tr>
<tr><td>E_2, kJ</td><td>68.944</td><td>n_1</td><td>1.89</td></tr>
<tr><td>E_3, kJ</td><td>68.830</td><td>n_2</td><td>0.60</td></tr>
<tr><td>$k_{1,\ mean}$</td><td>1.035e4</td><td>n_3</td><td>1.0</td></tr>
<tr><td>$k_{2,mean}$</td><td>9.210e5</td><td></td><td></td></tr>
<tr><td>$k_{3,mean}$</td><td>1.669e3</td><td></td><td></td></tr>
<tr><th colspan="4">Goodness of fit</th></tr>
<tr><td colspan="3">R^2</td><td>0.8892</td></tr>
<tr><td colspan="3">Std Err</td><td>0.1171</td></tr>
</table>
</td></tr>
</table>

Table 5.5. Model frameworks.

<table>
<tr><th>Model №</th><th>Model framework</th><th>Result of estimation</th></tr>
<tr><td>3</td><td>$\frac{dx_{FeS_2}}{dt}=\frac{(r_1+r_2)A_in}{c_{FeS_2,0}}$ $\frac{dc_{Fe^{3+}}}{dt}=-7r_2A_in\varepsilon+1/2r_3$
$\frac{dc_{Fe^{2+}}}{dt}=r_1A_in\varepsilon+15r_2A_in\varepsilon-r_3$ $\frac{dc_{L,O_2}}{dt}=0$
$r_1=k_1(1-x_{FeS_2})^{n_1}c^{*}_{L,O_2}{}^{n_2}$ where $k_1=k_{1,mean}\exp\left(-E_1/R\left(1/T-1/T_{mean}\right)\right)$
$r_2=k_2(1-x_{FeS_2})^{n_3}c^{n_4}_{Fe^{3+}}$ where $k_2=k_{2,mean}\exp\left(-E_2/R\left(1/T-1/T_{mean}\right)\right)$
$r_3=k_3c^2_{Fe^{2+}}c_{L,O_2}$ where $k_3=k_{3,mean}\exp\left(-E_3/R\left(1/T-1/T_{mean}\right)\right)$</td><td>
<table>
<tr><th colspan="4">Estimated Parameters</th></tr>
<tr><th>Parameter</th><th>Value</th><th>Parameter</th><th>Value</th></tr>
<tr><td>E_1, kJ</td><td>29.227</td><td>n_1</td><td>1.54</td></tr>
<tr><td>E_2, kJ</td><td>73.309</td><td>n_2</td><td>0.80</td></tr>
<tr><td>E_3, kJ</td><td>11.355</td><td>n_3</td><td>0.96</td></tr>
<tr><td>$k_{1,\,mean}$</td><td>1.492</td><td>n_4</td><td>1.86</td></tr>
<tr><td>$k_{2,mean}$</td><td>3.828e3</td><td></td><td></td></tr>
<tr><td>$k_{3,mean}$</td><td>4.263e5</td><td></td><td></td></tr>
<tr><th colspan="4">Goodness of fit</th></tr>
<tr><td colspan="3">R^2</td><td>0.9945</td></tr>
<tr><td colspan="3">Std Err</td><td>0.0260</td></tr>
</table>
</td></tr>
<tr><td>4</td><td>$\frac{dx_{FeS_2}}{dt}=\frac{(r_1+r_2)A_in}{c_{FeS_2,0}}$ $\frac{dc_{Fe^{3+}}}{dt}=-7r_2A_in\varepsilon+1/2r_3$
$\frac{dc_{Fe^{2+}}}{dt}=r_1A_in\varepsilon+15r_2A_in\varepsilon-r_3$ $\frac{dc_{L,O_2}}{dt}=0$
$r_1=k_1(1-x_{FeS_2})^{n_1}c^{*}_{L,O_2}{}^{0.5}$ where $k_1=k_{1,mean}\exp\left(-E_1/R\left(1/T-1/T_{mean}\right)\right)$
$r_2=k_2(1-x_{FeS_2})^{n_2}c^{n_3}_{Fe^{3+}}$ where $k_2=k_{2,mean}\exp\left(-E_2/R\left(1/T-1/T_{mean}\right)\right)$
$r_3=k_3c^2_{Fe^{2+}}c_{L,O_2}$ where $k_3=k_{3,mean}\exp\left(-E_3/R\left(1/T-1/T_{mean}\right)\right)$</td><td>
<table>
<tr><th colspan="4">Estimated Parameters</th></tr>
<tr><th>Parameter</th><th>Value</th><th>Parameter</th><th>Value</th></tr>
<tr><td>E_1, kJ</td><td>34.548</td><td>n_1</td><td>0.48</td></tr>
<tr><td>E_2, kJ</td><td>62.848</td><td>n_2</td><td>1.21</td></tr>
<tr><td>E_3, kJ</td><td>165.56</td><td>n_3</td><td>2.39</td></tr>
<tr><td>$k_{1,\,mean}$</td><td>3.041e-1</td><td></td><td></td></tr>
<tr><td>$k_{2,mean}$</td><td>5.584e4</td><td></td><td></td></tr>
<tr><td>$k_{3,mean}$</td><td>1.040e5</td><td></td><td></td></tr>
<tr><th colspan="4">Goodness of fit</th></tr>
<tr><td colspan="3">R^2</td><td>0.9946</td></tr>
<tr><td colspan="3">Std Err</td><td>0.0259</td></tr>
</table>
</td></tr>
</table>

5.6. Model frameworks.

<table>
<tr><th>Model №</th><th>Model framework</th><th colspan="4">Result of estimation</th></tr>
<tr><td rowspan="6">5</td><td rowspan="6">$\frac{dx_{FeS_2}}{dt}=\frac{(r_1+r_2)A_i n}{c_{FeS_2,0}}$ $\quad \frac{dc_{Fe^{3+}}}{dt}=-7r_2A_i n\varepsilon+1/2r_3$
$\frac{dc_{Fe^{2+}}}{dt}=r_1A_i n\varepsilon+15r_2A_i n\varepsilon-r_3$ $\quad \frac{dc_{L,O_2}}{dt}=0$
$r_1=k_1(1-x_{FeS_2})^{n_1}c^{*}_{L,O_2}{}^{0.5}$ where $k_1=k_{1,mean}\exp\left(-E_1/R\left(1/T-1/T_{mean}\right)\right)$
$r_2=k_2(1-x_{FeS_2})^{n_1}c^{n_2}_{Fe^{3+}}$ where $k_2=k_{2,mean}\exp\left(-E_2/R\left(1/T-1/T_{mean}\right)\right)$
$r_3=k_3c^2_{Fe^{2+}}c_{L,O_2}$ where $k_3=k_{3,mean}\exp\left(-E_3/R\left(1/T-1/T_{mean}\right)\right)$</td><td colspan="4">Estimated Parameters</td></tr>
<tr><td>Parameter</td><td>Value</td><td>Parameter</td><td>Value</td></tr>
<tr><td>E_1, kJ</td><td>33.745</td><td>n_1</td><td>0.72</td></tr>
<tr><td>E_2, kJ</td><td>91.012</td><td>n_2</td><td>1.59</td></tr>
<tr><td>E_3, kJ</td><td>10.03</td><td></td><td></td></tr>
<tr><td>$k_{1,\ mean}$</td><td>3.092e-1</td><td></td><td></td></tr>
<tr><td>$k_{2,mean}$</td><td>3.571e2</td><td></td><td></td></tr>
<tr><td>$k_{3,mean}$</td><td>1.591e5</td><td></td><td></td></tr>
<tr><td colspan="4">Goodness of fit</td></tr>
<tr><td colspan="3">R^2</td><td>0.9948</td></tr>
<tr><td colspan="3">Std Err</td><td>0.0253</td></tr>
</table>

5.3.3 Predictions of models

The results of the simulations and the analysis of the reliability of the models and their parameters are collected in this chapter. The estimated parameters and the goodness of the fit are introduced in Table 5.4 and Table 5.5. The results of the MCMC analysis for each model are shown below presenting two-dimensional posterior distributions for the parameters. The density of the dots in each figure represents probability. The elongated probability region on figures between two parameters means that there is a considerable cross-correlation between these parameters. The correlation coefficients between the parameters allows to evaluate the extent of cross-correlation in a numerical way.

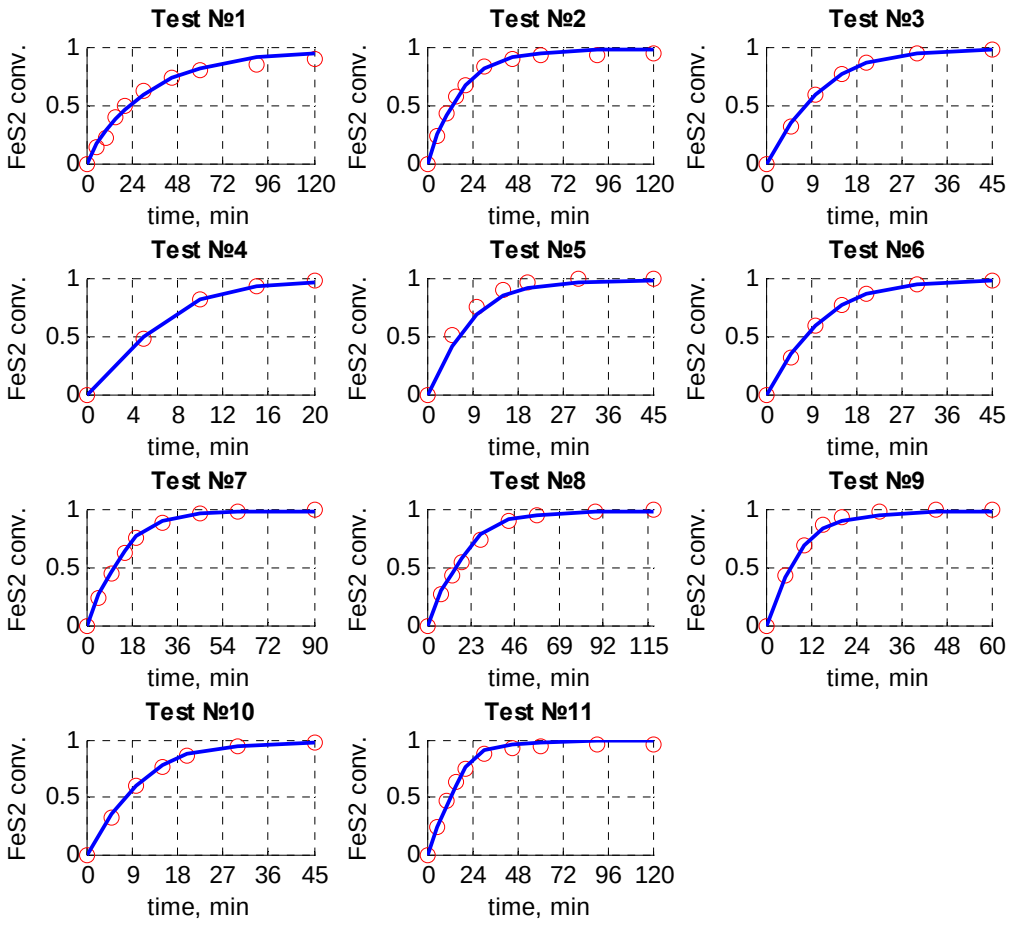

Figure 5.3. **Model 1**. Experimental data and model prediction (solid lines) at various conditions.

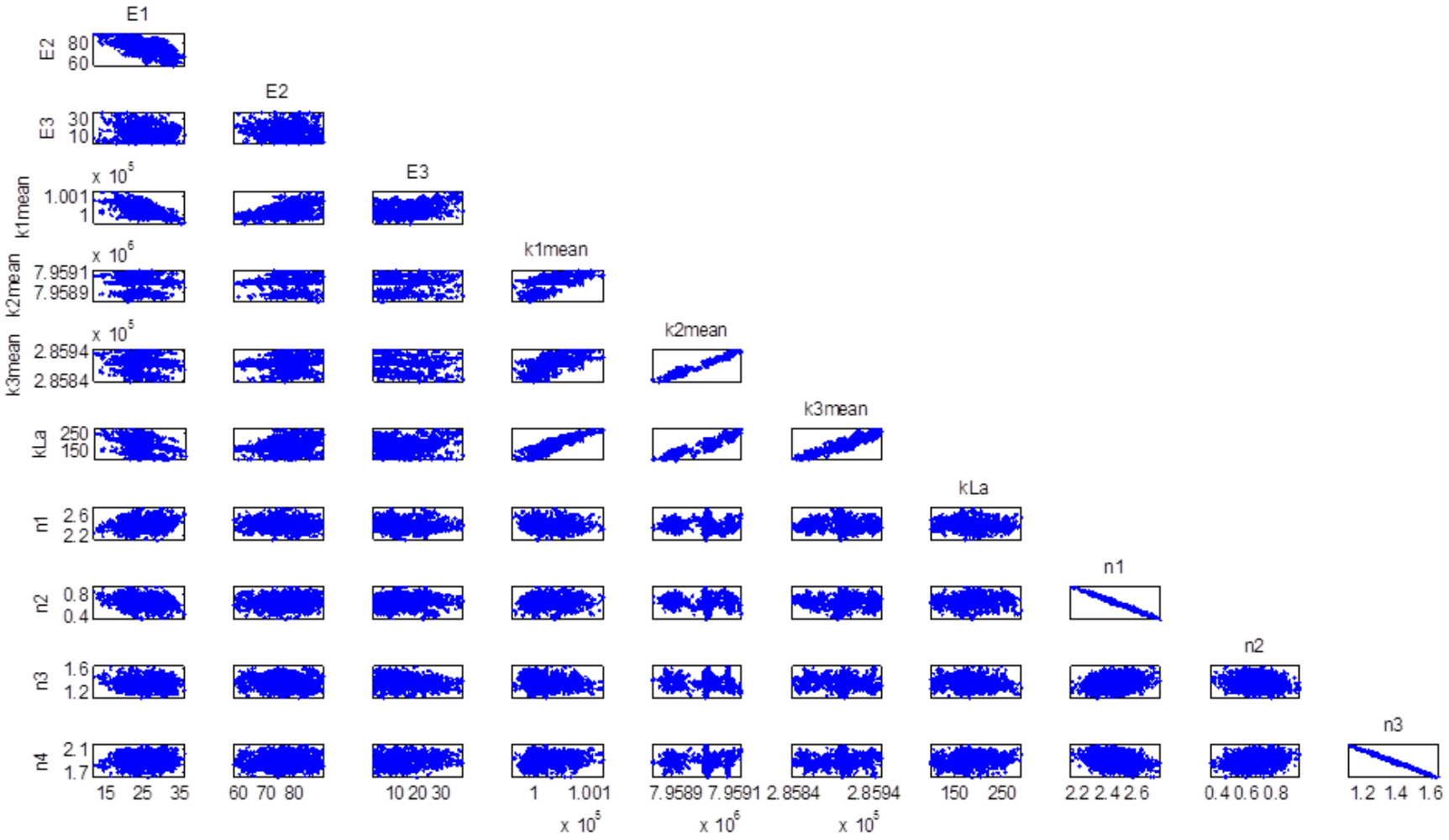

Figure 5.4. **Model 1**. Results of the MCMC analysis.

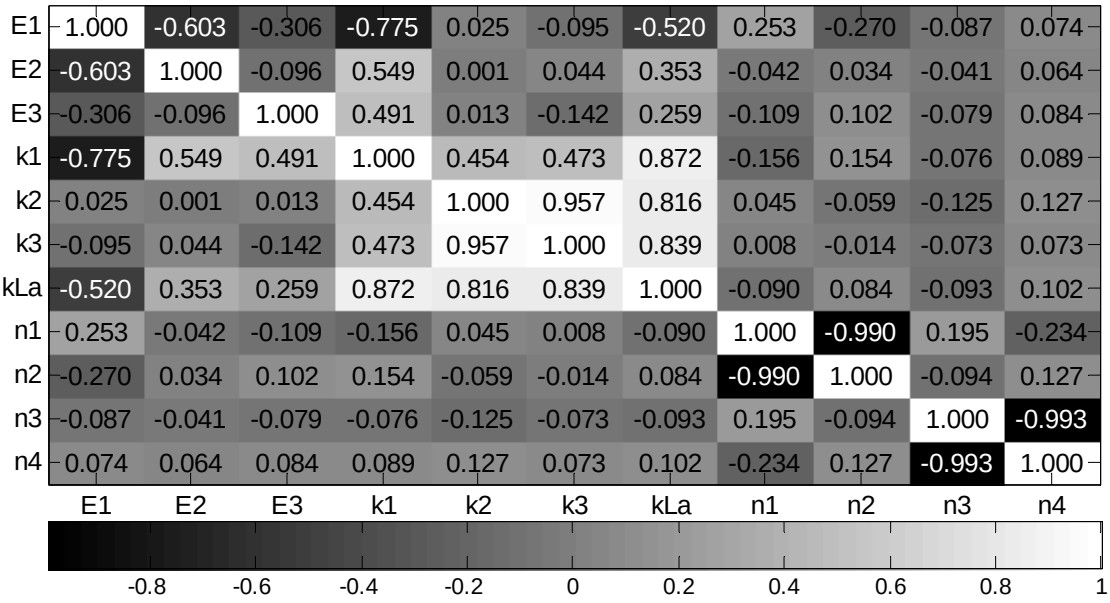

Figure 5.5. **Model 1**. Correlation matrix.

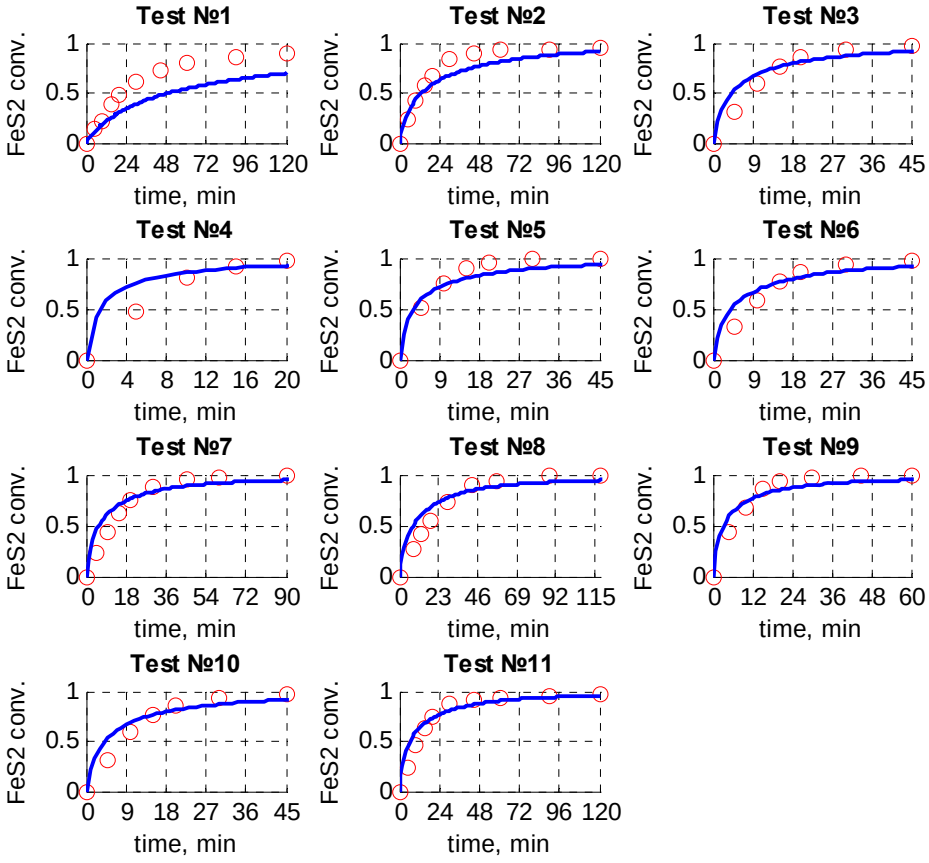

Figure 5.6. **Model 2.** Experimental data and model prediction (solid lines) at various conditions.

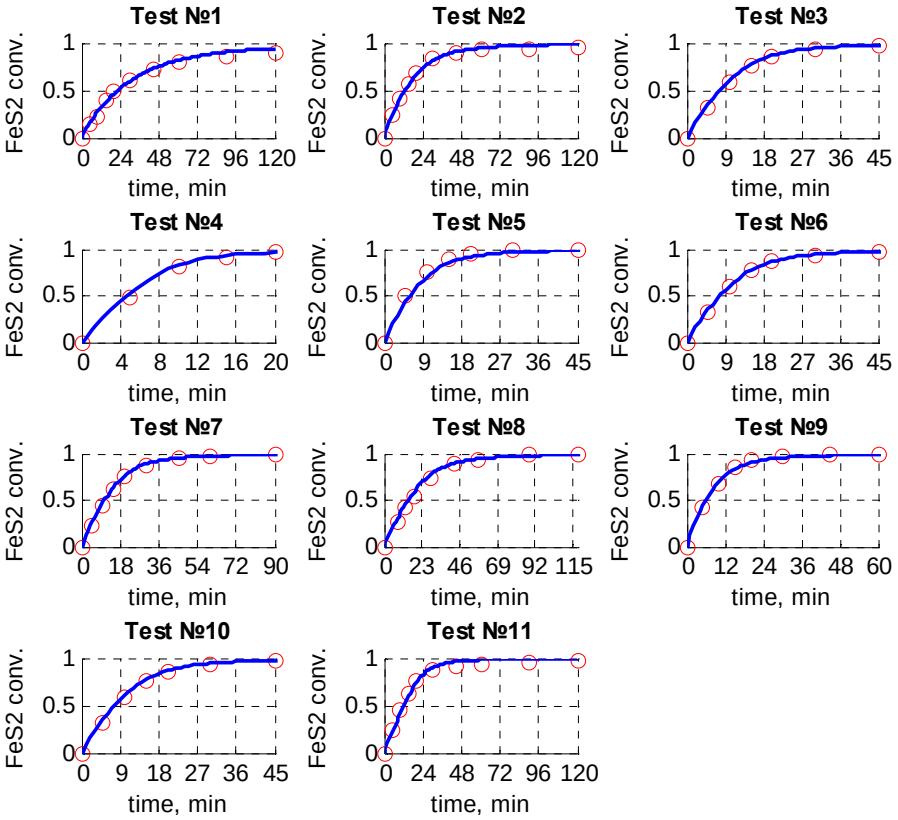

Figure 5.7. **Model 3.** Experimental data and model prediction (solid lines) at various conditions.

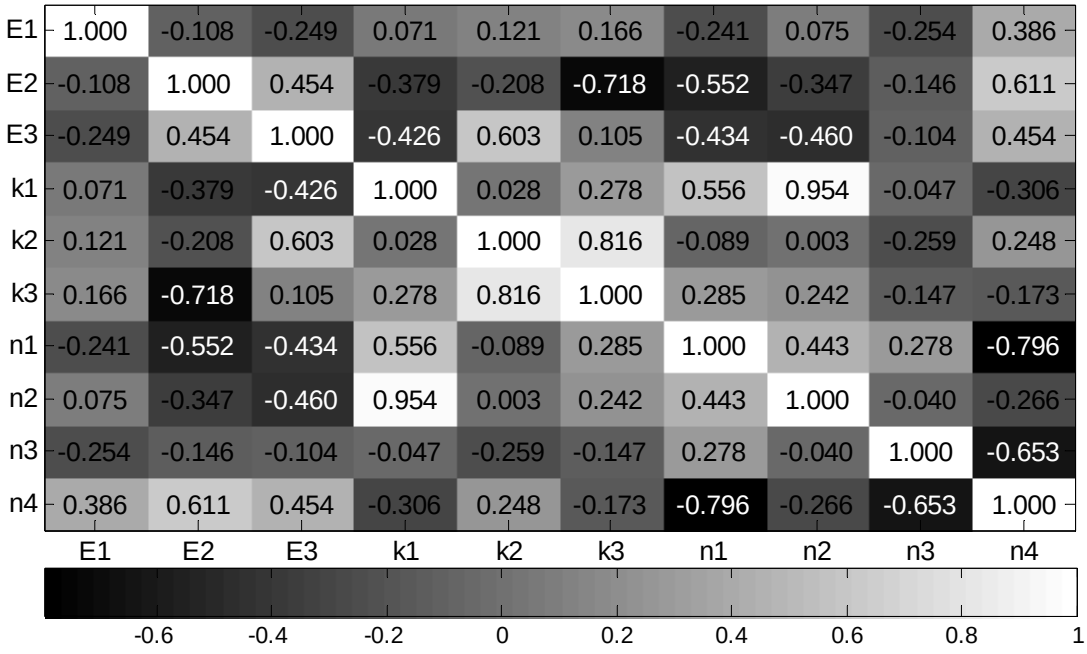

Figure 5.8. **Model 3**. Correlation matrix.

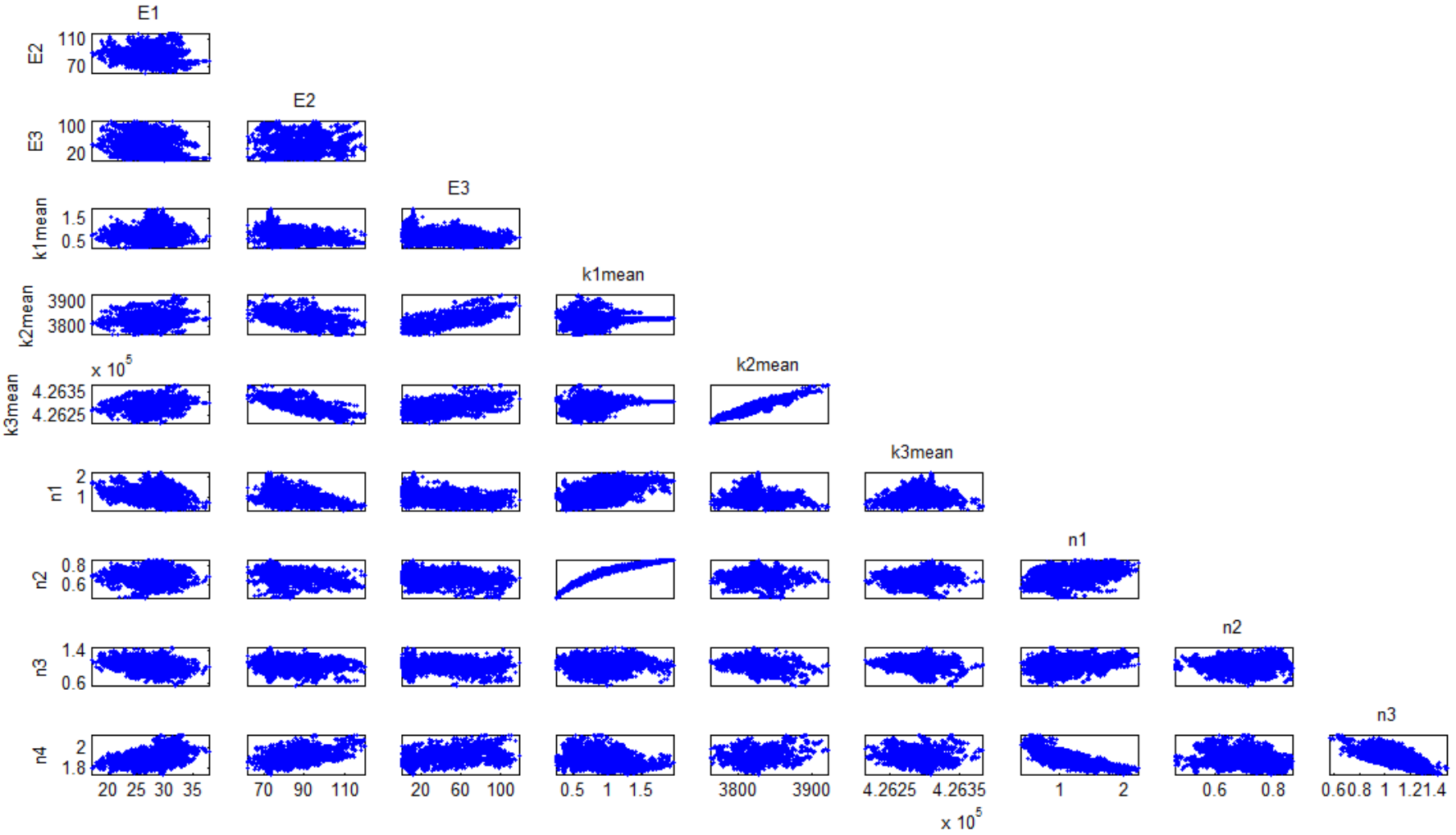

Figure 5.9. **Model 3**. Results of the MCMC analysis.

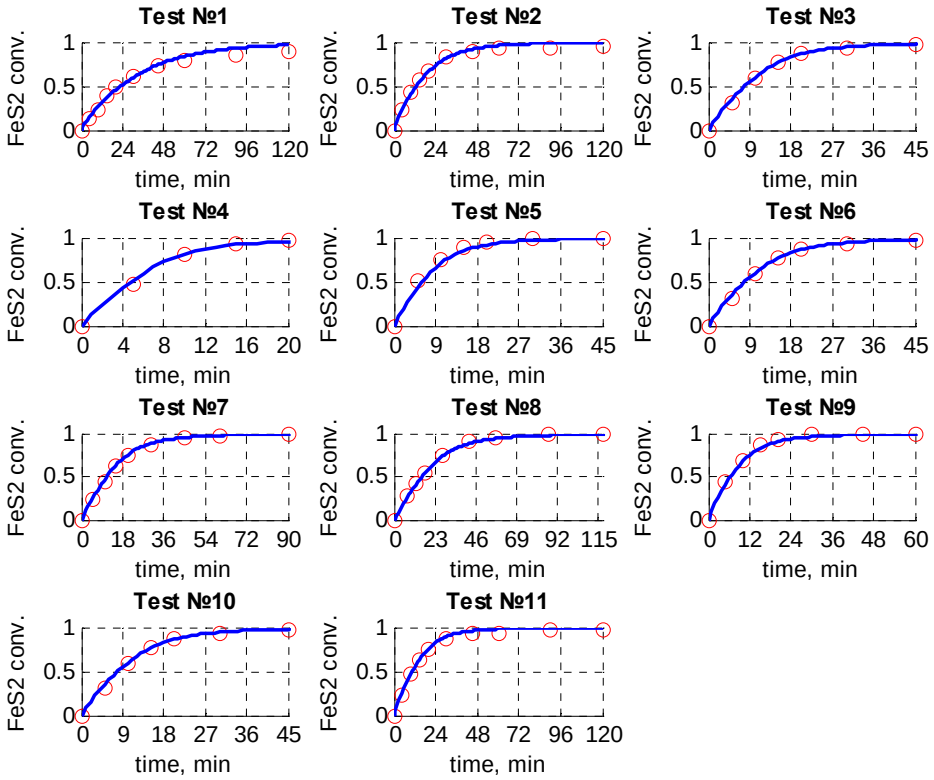

Figure 5.10. **Model 4**. Experimental data and model prediction (solid lines) at various conditions.

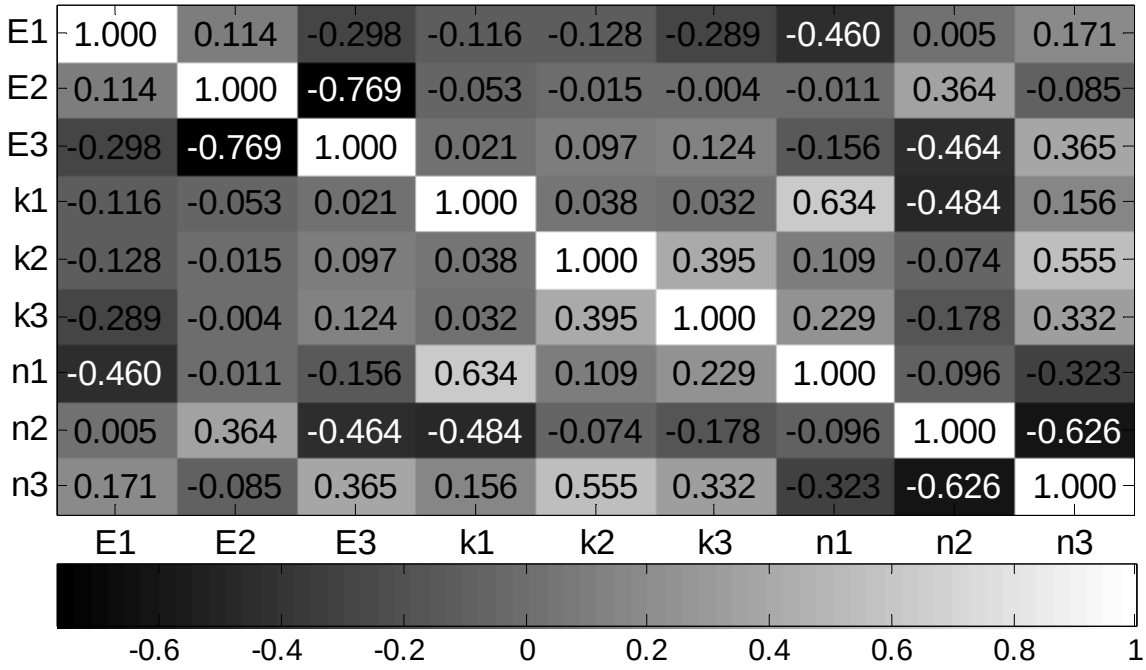

Figure 5.11. **Model 4**. Correlation matrix.

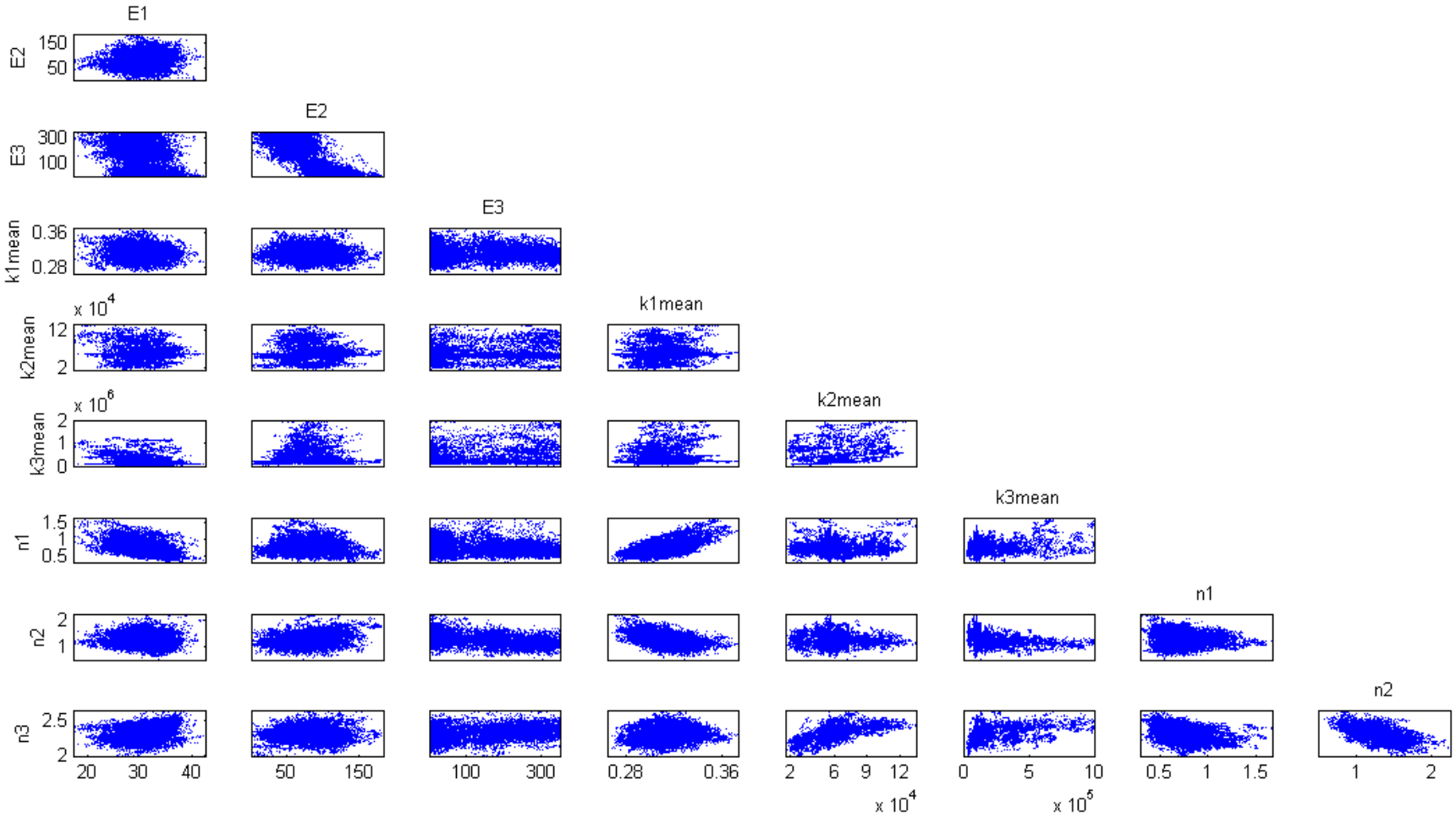

Figure 5.12. **Model 4**. Results of the MCMC analysis.

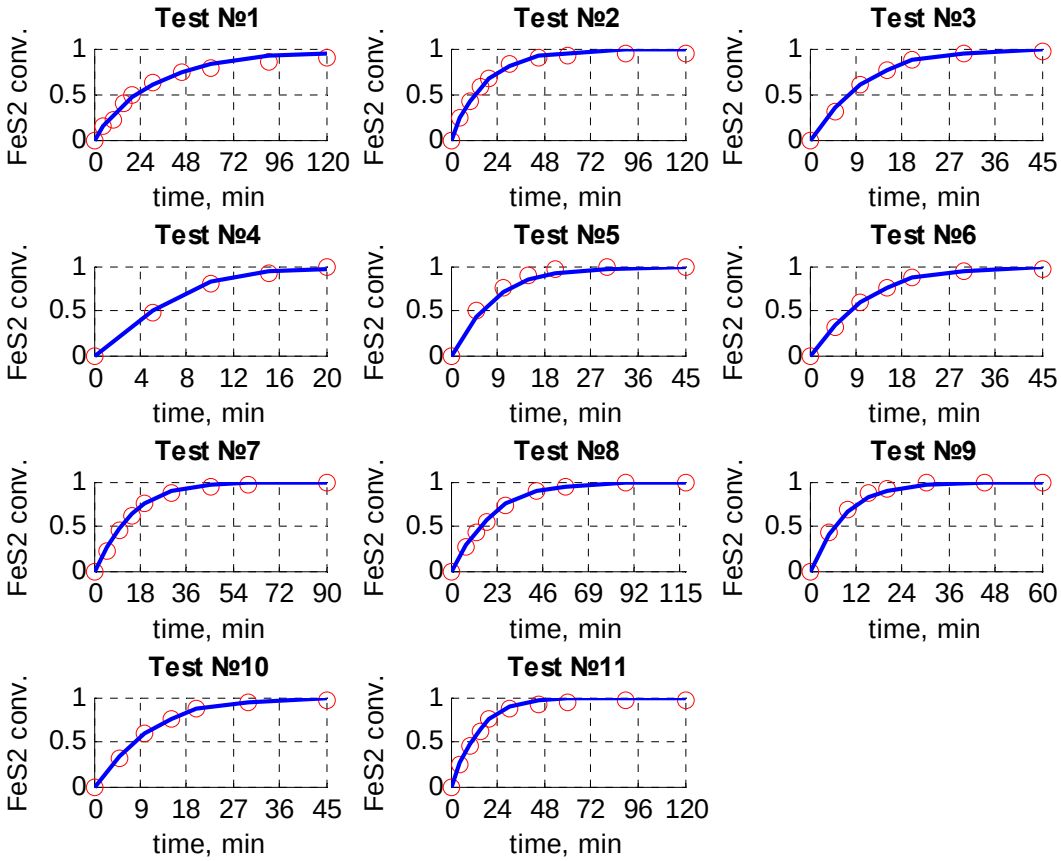

Figure 5.13. **Model 5**. Experimental data and model prediction (solid lines) at various conditions.

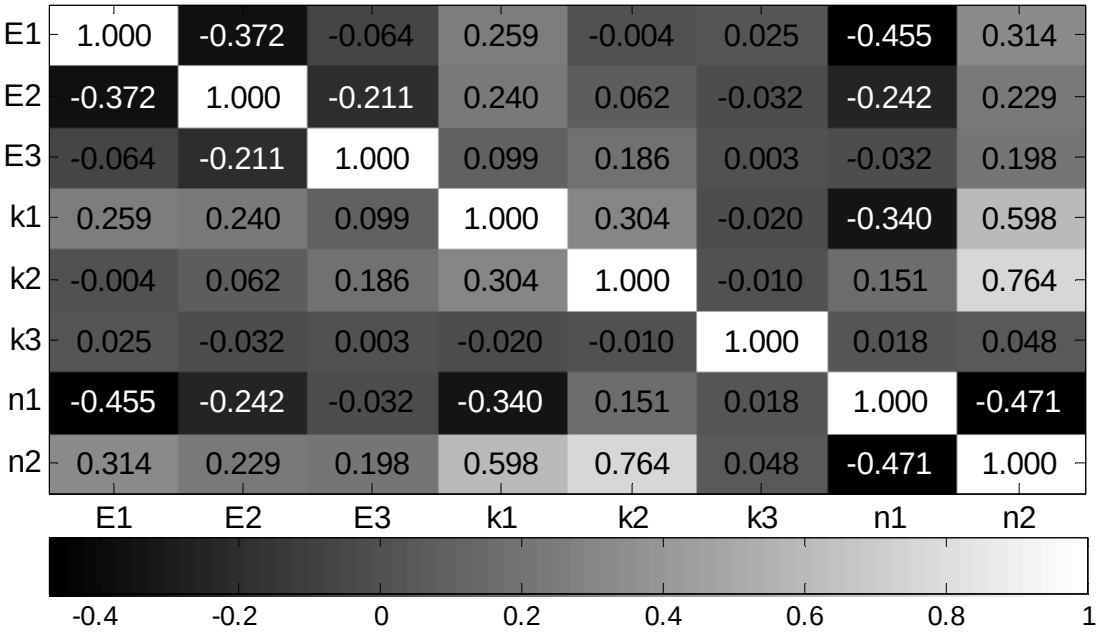

Figure 5.14. **Model 5**. Correlation matrix.

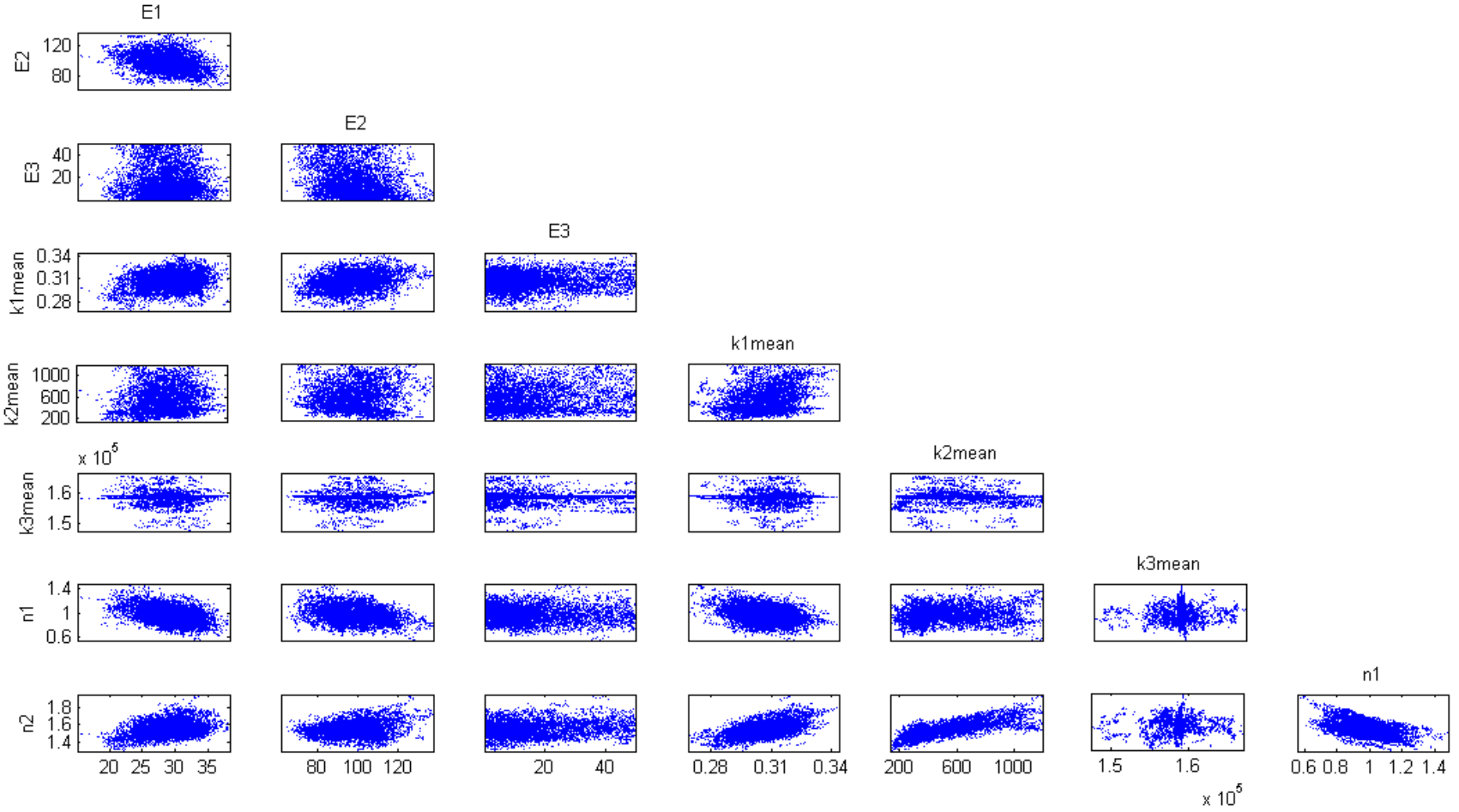

Figure 5.15 **Model 5**. Results of the MCMC analysis.

6 DISCUSSIONS

The oxidation kinetics of a pyrite ore in sulfuric acid solution under oxygen pressure was investigated by creating a descriptive mathematical model. The model implementation based on initial assumptions about the mechanism of oxidation process:

- solid particles of pyrite are treated as a pseudo-homogeneous phase;

- pyrite oxidation kinetics are limited by the rate of reaction at the pyrite surface;

- pyrite concentration at the reactive surface is a characteristics for the concentrate and can be assumed to remain constant during oxidation;

- the relationship between mean particle size and conversion can be described by the shrinking core model;

- the oxidation rate depends on the mass transfer of oxygen to the mineral surface which is principally a function of the dissolved oxygen concentration, partial pressure, and temperature. The molal concentration of dissolved oxygen is given by Tromans' model (Tromans, 1998).

- passivation of the mineral surface should be taken into account due to deviations at higher conversions which are obtained by using the shrinking sphere model;

- the passivation effect are expressed by introducing a "passivation term" into the rate of pyrite oxidation: $(1 - x_{FeS_2})^n$;

- passivation influences the pyrite oxidation in different ways, thus, the distinct extent of the "passivation term" for oxygen and ferric oxidation paths;

These statements are implemented in Model 1 and Model 2. The difference between them is that Model 2 assumes equal impact of passivation phenomena on pyrite oxidation rate. Thus the parameters n_1 and n_3 for Model 2 were estimated as equal. A number of conclusions may be drawn from the results of parameters estimation for Model 1 and Model 2 (see results at Figures 5.3, 5.4, 5.5, and 5.6):

- the best fit was obtained by using Model 1 ($R2_{Model1}$ = 0.9943 while $R2_{Model2}$=0.8892);

- the order for the reaction rate of pyrite dissolution by oxygen seems to be close and do not exceed 1.0 (half-order is reported by literature sources);

- the activation energy for each rate equation in Model 1 do not exceed 80 kJ, that could indicate that the reaction is chemically controlled;

- Model 1 shows that the exponent of the "passivation term" for pyrite oxidation by oxygen is almost twice larger compared to corresponding term for ferric ions.

- the results of the MCMC analysis (Figure 5.4) for Model 1 and the correlation matrix (Figure 5.5) show a strong correlation (0.872, 0.816, and 0.839) between the mass transfer coefficient (k_La) and the pre-exponential factors (k_{1mean}, k_{2mean}, k_{3mean}).

The mass transfer coefficient is specific to each reactor and therefore is complicated to predict. The value of k_La could vary depending on the hydrodynamics and have a large impact on the performance of the process if it was operating in the mass transfer controlled regime. In that case, agitation speed is important in liquid-solid reactions. Long and Dixon (2004) mentioned that agitation speed had no considerable effect on the initial rate of pyrite oxidation when maintained at 800 rpm of higher (for the used experimental data the agitation speed was 800 rpm). Thus, k_La can be removed from the estimated parameters assuming that the concentration of the dissolved oxygen equals the

saturation concentration. Models 3, 4, and 5 take into account this assumption. Moreover, for Model 4 and Model 5 it is assumed that pyrite oxidation exhibits a 0.5-order dependency on dissolved oxygen concentration. A number of conclusions may be drawn from the results of the parameters estimation for Model 3 and Model 4 (see results at Figures 5.7, 5.8, 5.9, 5.10, 5.11, and 5.12):

- both models give a relatively good fit ($R2_{Model3}$=0.9945 and $R2_{Model4}$=0.9946);

- the MCMC analysis for Model 3 shows a strong correlation between the pre-exponential factor k_{1mean} and parameter n_2 (oxygen order);

- elimination of parameter n_2 gives a relatively good estimation with maximum correlation factor less than 0.8.

Although the earlier Model 2, which assumes an equal impact of the passivation phenomena on pyrite oxidation rate, demonstrated R^2 value less than for Model 1 (0.8892 against 0.9943), this assumption was checked for Model 4. Thus, Model 5 with eight parameters takes into account equal impact of passivation phenomena by a common parameter n_1. Estimation of parameters for Model 5 gives similarly good results compared to Model 1, Model 3 and Model 4. That means that each model could give a relatively good fit (the structure of each model is similar, but the exponents are varied), but the used algorithm of estimation have a high dependence on initial guesses. Thus, for models which have less variable parameters it is easier to find initial parameter values giving right the direction for the fitting procedure. Another problem which could appear in the case of large number of parameters is the high correlation between them.

Another question which can appear is the meaning of the exponents for the "passivation term" ($(1-x_{FeS_2})^n$). The distinct extent of the "passivation term" (for Model 1, 3, and 4) is unclear. On the other hand equal impact of passivation can be explained by introducing a shape factor.

As was shown above for Model 5:

$$\frac{dx_{FeS_2}}{dt} = \frac{(r_1 + r_2) A_i n}{c_{FeS_2,0}} \quad (23)$$

$$r_1 = k_1 (1 - x_{FeS_2})^{n_1} c_{L,O_2}^{0.5} \quad (24) \quad \text{and} \quad r_2 = k_2 (1 - x_{FeS_2})^{n_1} c_{Fe^{3+}}^{n_2} \quad (25)$$

$$\text{where } A_i = \pi (1 - x_{FeS_2})^{2/3} d_0^2 \quad (26)$$

the rate equations can be transformed into the form:

$$\frac{dx_{FeS_2}}{dt} = \frac{(r_1 + r_2) \pi (1 - x_{FeS_2})^{2n_1} d_0^2 \, n}{c_{FeS_2,0}} \quad (27)$$

$$\text{where } r_1 = k_1 c_{L,O_2}^{0.5} \quad (28) \quad \text{and} \quad r_2 = k_2 c_{Fe^{3+}}^{n_2} \quad (29)$$

thus, the shrinkage of the particle core is described by the following equation:

$$\left(\frac{d_i}{d_o} \right)^{\psi} = 1 - x_{FeS_2} \quad (30)$$

where parameter ψ is a shape factor (equal 1/3≈0.333 for spherical particles) which was estimated for Model 5 as 0.693.

7 CONCLUSIONS

A mathematical model was developed for pyrite oxidation kinetics in a batch reactor under acidic conditions at high pressure and temperature. The model takes into account the effects of temperature, oxygen pressure, gas-liquid oxygen mass transfer rate and particle size on the reaction kinetics.

The reaction rates are described as surface reactions taking place at the surface of pyrite particles. The decrease of the surface area is described by the shrinking core model where the active surface area is calculated from pyrite conversion.

The five different kinetic models were tested including different number of parameters. In the most complete form the model has 11 parameters, activation energies E_1, E_2 and E_3, rate constants at mean temperature, k_{1mean}, k_{2mean}, k_{3mean}, volumetric gas-liquid mass transfer coefficient k_La, exponents for pyrite passivation n_1 and n_2 and reaction orders for oxygen n_2 and ferric iron n_4. The reasons of elimination of some parameters were discussed above. The model parameters were estimated by comparing the model predictions to literature data. For all models a reasonably good fit (R2 > 88 %) was obtained.

The reliability of the models was evaluated by MCMC analysis. According to the results the reliability of the most complete model is questionable due to correlations between the parameters. The reliability of the model is improved when the volumetric mass transfer coefficient is removed from the estimated parameters assuming saturated oxygen concentration in the liquid phase. Moreover, it is assumed that pyrite oxidation exhibits a 0.5-order dependency on dissolved oxygen concentration. Thus, eight parameters seem to be enough for successful estimation. It was noticed that each model give relatively good fit to the experimental data, but the extent of cross-correlation between the parameters is different. Finally, the "passivation term" for pyrite oxidation (for both, by oxygen and by ferric ions) can be replaced by a shape factor which is estimated as a result of the fitting procedure.

REFERENCES

Abrantes, L. M. and Costa, M. C. 2004. Electro-oxidation as a pre-treatment for gold recovery. *Hydrometallurgy.* 2004, Vol. 40, 1-2, pp. 99-110.

Bailey, L. K. and Peters, E. 1976. Decomposition of pyrite in acids by pressure leaching and anodization: the case for an electrochemical mechanism. *Canadian Metallurgical Quarterly.* 15, 1976, Vol. 4, pp. 333-344.

Baldwin, S. A., Demopoulos, G. P. and Papangelakis, V. G. 1995. Mathematical modeling of the zinc pressure leach process. *Metallurgical and Materials Transactions B.* 5, 1995, Vol. 26, pp. 1035-1047.

Baldwin, Susan A. and Demopoulos, George P. 1998. Parameter sesitivity of kinetics-base hydrometallurgical reactor models. *The canadian journal of chemicla engineering.* 1998, Vol. 76, 6, pp. 1083-1092.

Bhappu, Roshan B. 1990. Hydrometallurgical processing of precious metal ores. *Mineral Processing and Extractive Metallurgy Review: An International Journal.* 1990, Vol. 6, 1-4, pp. 67-80.

Boyle, R. W. 1980. *The geochmeistry of gold and its deposits.* s.l. : Unipub, 1980. Vol. 280.

Carrillo-Pedroza, F. R., Soria-Aduilar, M. J. and Salinas-Rodriguez, E. 2012. Oxidative Hydrometallurgy of Sulphide Minerals. [book auth.] Mohammad Nusheh. *Recent Researches in Metallurgical Engineering - From Extraction to Forming.* 2012, pp. 25-42.

Crundwel, F. K. 1995. Progress in the mathematical modelling of leching reactors. *Hydrometallurgy.* 1995, Vol. 39, 1-3, pp. 321-335.

Derry, R. 1972. *Pressure hydrometallurgy; a bibliographical review.* Hertfordshire, UK : Warren Spring Laboratory, Dep. of Trade and Industry, 1972. Vol. 7.

Developments in the pretreatment of refractory gold minerals by nitric acid. **Li, D. X. 2009.** 2009. pp. 145-150.

Duncan, Turner W. 2000. *Albion process for treatment of refractory ores.* Australia : s.n., 2000.

Dunne, R. 2005. Flotation of gold and gold-bearing ores. [book auth.] M. D. Adams. *Advances in Gold Ore Processing.* 2005.

Elvers, B., Hawkins, S. and Ravenscraft, M., [ed.]. 1990. *Ullman´s Encyclopedia of Industrial Chemistry.* 5. Weinheim : s.n., 1990.

Garrels, R. M. and Thompsom, M. E. 1960. Oxidation of pyrite by iron sulfate solutions. *Am. J. Sci.* 1960, Vol. 258A, pp. 57-67.

Gasparrini, C. 1983. The mineralogy of gold and its significance in metal extraction. *CIM Bull.* 1983, Vol. 76, pp. 144-153.

Gudyanga, F. P., Mahlangu, T. and Roman, R. J. 1999. An acidic pressure oxidation pre-treatment of refractory gold concentrates from the Kwekwe roasting plant. 1999, Vol. 12, 8, pp. 863-875.

Haario, H., et al. 2006. DRAM: Efficient adaptive MCMC. *Statistics and Computing.* 2006, 16, pp. 339-354.

Haario, H., Saksman, E. and Tamminen, J. 2001. An adaptive Metropolis algorithm Benoulli. 2001, 7, pp. 223-242.

Habashi, F. 1999. *Text book of Hydrometallurgy.* Quebec : Metallurgie Extractive Quebec, 1999.

Harris, D. C. 1990. The mineralogy of gold and its relevance to gold recoveries. *Mineralium deposita.* 1990, Vol. 25, 1, pp. S3-S7.

Holmes, Paul R. and Crundwell, Frank K. 2000. The kinetics of the oxidation of pyrite by ferric ions nad dissolved oxygen: An electrochemical study. *Geochemica et Cosmochimica Acta.* 2000, Vol. 64, 2, pp. 263-274.

Lampinen, Matti, Laari, Arto and Turunen, Ilkka. 2010. Simulation of direct leaching of zinc concentrate in a non-ideally mixed CSTR. *The canadian journal of chemical engineering.* 2010, Vol. 88, 4, pp. 625-632.

Leons Eugene, W. W. and Mujumdar, A. S. 2009. *Gold Extraction and Recovery Processes.* s.l. : National University of Singapore, 2009.

Levenspiel, Octave. 1999. *Chemical reaction engineering.* USA : John Wiley & Sons, Inc., 1999.

Lodejshhikov, V. V. 2008. Some possibilities for processing refractory gold ores. *Gold mining.* 2008, Vol. 117. (In Russian).

—. Irkutsk. *Technology to extract gold and silver from refractory ores.* 1999 : Public Traded Company Irgiredmet, Irkutsk. (In Russian).

Long, Hu and Dixon, David G. 2004. Pressure oxidation of pyrite in sulfuric acid media: a kinetic study. *Hydrometallurgy.* 2004, Vol. 73, 3-4, pp. 335-349.

Lowson, Richard T. 1982. Aqueous oxidation of pyrite by molecular oxygen. *Chemical Reviews.* 1982, Vol. 82, 5, pp. 461-497.

Lucik, V. I. and Sobolev, A. E. 2009. *Kinetics of hydrolytic and oxidative dissolution of metal sulfides: Monograph.* Tver' : TGTU, 2009. (In Russian).

Marsden, John O. and House, Iain C. 2006. *The Chemistry of Gold Extraction.* Colorado, USA : Society for Mining, Metallurgy, and Exploration, Inc., 2006.

McDonald, R. G. and Muir, D. M. 2007. Pressure oxidation leaching of chalcopyrite. Part I. Comparison of high and low temperature reaction kinetics and products. *Hydrometallurgy.* 2007, Vol. 86, 3-4, pp. 191-205.

McKay, D. R. and Halpern, J. 1957. *A kinetic study of the oxidation of pyrite in aqueous suspension.* s.l. : University of British Columbia, 1957.

McKibben, M. A. and Barnes, H. L. 1986. Oxidation of pyrite in low temperature acidic solutions: rate laws and surface textures. *Geochim. Cosmochim. Acta.* 1986, 50.

—. 1986. Oxidation of pyrite in low temperature acidic solutions: rate laws and surface textures. *Geochim. Cosmochim. Acta.* 1986, Vol. 50, pp. 1509-1520.

Mukherjee, T. K., et al. 1985. Chloridizing roasting process for a complex sulfide concentrate. *Journal of metals.* 1985, Vol. 37, 6.

Naboichenko, S. S., et al. 2009. *Autoclave hydrometallurgy of nonferrous metals.* Ekaterinburg : s.n., 2009. (In Russian).

Neuvonen, Marija. 2013. *Pretreatent processes in gold recovery by thiosulphate leaching.* Lappeenranta : s.n., 2013.

Non-ferrous metallurgy. **Hrjashhev, S. V. and Berezkin, O. P. 1967.** 1967, Vols. 22, 23. (In Russian).

Nowak, P. 2001. On the rate equation of the oxidative dissolution of metal sulfides. *Transactions of the Strata Mechanics Research Institute.* 2001, Vol. 3.

Papangelakis, V. G. and Demopoulos, G. P. 1991. Acid pressure oxidation of pyrite: reaction kinetics. *Hydrometallurgy.* 1991, Vol. 26, 3, pp. 309-325.

—. 1992. On the attaiment of stable autothermal operation in continuos pressure leaching reactors. *Hydrometallurgy.* 1992, Vol. 29, 1-3, pp. 297-318.

—. 1992. Reactor models for a series of continuous stirred tank reactors with a gas-liquid-solid leaching system: Part III. Model application. *Metallurgical Transactions B.* 1992, Vol. 23, 6, pp. 865-877.

—. 1992. Reactor models for a series of continuous stirred tank reactors with a gas-liquid-solid leaching systems: Part I. Surface reaction control. *Metallurgical Transactions B.* 1992, Vol. 23, 6, pp. 847-856.

—. 1992. Reactor models for a series of continuous strirred tank reactors with a gas-liquid-solid leaching system: Part II. Gas transfer control. *Metallurgical Transactions B.* 1992, Vol. 23, 6, pp. 857-864.

Papangelakis, V. G., Berk, D. and Demopouls, G. P. 1990. Mathematical modeling of an exothermic leaching reaction system: pressure oxidation of wide size arsenopyrite particles. *Metallurgical Transactions B.* 1990, Vol. 21, 5, pp. 827-837.

Rubisov, D. H. and Papangelakis, V. G. 1996. Mathematical modelling of the transient behaviour of CSTRs with reactive particulates: Part 2 - Application to pyrite pressure oxidation. *Can. J. Chem. Eng.* 1996, Vol. 74, 3, pp. 363–371.

Rusanen, L., Aromaa, J. and Forsen, O. 2013. Pressure oxidation of pyrite-arsenopyrite refractory gold concentrate. *Physicochemical Problems of Mineral Processing.* 2013, Vol. 49, 1, p. 101.

Sato, M. 1960. Oxidation of sulfide ore bodies. II. Oxidation mechanisms of sulfide minerals at 25 0C. *Economic Geology.* 1960, Vol. 55, pp. 1202-1231.

Sepulveda, J. E. and Herbs, J. 1979. A population balance approach to the modelling of multistage continuous leaching systems. *AIChE Symposium Series.* 1979, Vol. 57, pp. 173-185.

Shneerson , Ja. M, Chugaev , L. V. and Pleshkov , M. A. Autoclave technology in Russia. *vnedra.ru.* [Online] [Cited: 6 17, 2013.] (In Russian). http://vnedra.ru/%D0%B0%D0%B2%D1%82%D0%BE%D0%BA%D0%BB%D0%B0%D0%B2%D0%BD%D1%8B%D0%B5-%D1%82%D0%B5%D1%85%D0%BD%D0%BE%D0%BB%D0%BE%D0%B3

%D0%B8%D0%B8-%D0%B2-
%D1%80%D0%BE%D1%81%D1%81%D0%B8%D0%B8-1088/.

Singer, P. C. and Stumm, W. 1970. Acid mine drainage: The rate limiting step. *Science.* 1970, Vol. 167, pp. 1121-1123.

Smith, H. 2005. Process simulation and modeling. [book auth.] Mike D. Adams. *Developments in mineral processing.* 2005.

Sobel, K. I. and Foo, K. A. 1995. Pilot plant evaluation of the redox process for Bakyrchik Gold Plc. 1995, Vol. 8, 4-5, pp. 431-440.

Thomas, K. G. 2005. Pressure oxidation overview. [book auth.] M. D. Adams. *Advances in Gold Ore Processing.* 2005, Vol. 15.

Tromans, Desmond. 1998. Oxygen solubility modeling in inorganic solutions: concentration, temperature and pressure effects. *Hydrometallurgy.* 1998, Vol. 50, 3, pp. 279-296.

—. 1998. Temperature and pressure dependent solubility of oxygen in water: a thermodynamic analysis. *Hydrometallurgy.* 1998, Vol. 48, 3, pp. 327-342.

Vaughan, J. P. 2004. The process mineralogy of gold: the classification of ore types. *Journal of metals.* 2004, Vol. 56, 7, pp. 46-48.

Williamson, M. A. and Rimstidt, J. D. 1984. Rates of reaction of pyrite and marcasite with ferric ion at pH 2. *Geochim. Cosmochim. Acta.* 1984, Vol. 48, 1, pp. 85-92.

—. 1994. The kinetics and electrochemical rate-determining step of aqueous pyrite oxidation. *Geochimica et Cosmochimica Acta.* 1994, Vol. 58, 24, pp. 5443–5454.

APPENDICES

Appendix I: Set of experimental data

Appendix I, 1(1)

Set of experimental data

Table I. Effect of temperature on pyrite oxidation (Long, et al., 2004).

Parameters of experiment												
d_{mean}, μm						62.6						
P_{O2}, kPa						690						
$[FeS_2]$, g/L						1						
$[H_2SO_4]$, M						0.5						
Results of experiment												
Temp.	230^0C			210^0C			190^0C			170^0C		
Time, min	Conv., %	d/d_0	Fe^{3+}/Fe_{tot}	Conv., %	d/d_0	Fe^{3+}/Fe_{tot}	Conv., %	d/d_0	Fe^{3+}/Fe_{tot}	Conv., %	d/d_0	Fe^{3+}/Fe_{tot}
0	0.0	1.00	0.0	0.0	1.00	0.0	0.0	1.00	0.0	0.0	1.00	0.0
5	47.7	0.81	58.8	31.6	0.88	64.0	23.2	0.90	67.6	14.0	0.95	67.6
10	80.9	0.58	61.1	59.1	0.74	45.3	42.2	0.82	38.5	25.5	0.91	39.5
15	92.1	0.43	76.6	76.6	0.62	58.3	57.3	0.74	47.8	39.1	0.85	43.4
20	97.8	0.28	80.7	86.5	0.51	75.6	67.5	0.68	49.8	48.9	0.80	43.0
30			81.7	93.7	0.40	78.9	83.6	0.54	59.0	61.5	0.73	31.2
45			82.6	97.1	0.31	80.1	89.7	0.46	61.6	73.0	0.65	38.0
60			82.6			80.9	93.0	0.40	67.4	79.3	0.59	43.7
90			82.7			80.9	93.5	0.39	71.1	85.1	0.53	50.0
120			82.7			81.1	94.9	0.36	77.7	89.7	0.47	61.1

Table II. Effect of particle size on pyrite oxidation (Long, et al., 2004).

Parameters of experiment													
Temperature, ^{0}C						210							
P_{O2}, kPa						690							
$[FeS_2]$, g/L						1							
$[H_2SO_4]$, M						0.5							
Results of experiment													
d_{mean}, μm	48.3			62.6			88.1			125.1			
Time, min	Conv., %	d/d_0	Fe^{3+}/Fe_{tot}	Conv., %	d/d_0	Fe^{3+}/Fe_{tot}	Conv., %	d/d_0	Fe^{3+}/Fe_{tot}	Fe^{3+}/Fe_{tot}	Time, min	Conv., %	d/d_0
0	0.00	1.00	0.0	0.00	1.00	0.0	0.00	1.00	0.0	0.0	0	0.0	1.00
5	50.17	0.80	46.7	31.74	0.88	64.1	23.04	0.91	67.3	80.1	7.8	27.3	0.90
10	75.26	0.63	73.4	59.22	0.74	45.3	44.20	0.82	50.9	56.0	12.8	42.0	0.83
15	89.25	0.48	79.6	76.79	0.62	58.4	62.46	0.71	44.8	43.8	17.8	53.8	0.77
20	95.39	0.36	81.8	86.52	0.51	75.6	74.74	0.62	66.3	61.3	27.8	73.9	0.64
30	98.63	0.24	83.0	93.69	0.40	79.0	87.54	0.49	75.6	70.4	42.8	89.8	0.47
45	100.00	0.11	83.6	96.93	0.31	80.1	95.22	0.35	77.5	76.3	57.7	94.0	0.39
60			84.7			80.9	97.27	0.28	79.9	78.5	87.8	98.3	0.26
90			85.2			81.1	99.32	0.11	80.1	77.7	117.8	99.0	0.23
120			85.3			81.1			81.1	78.7			

Table III. Effect of oxygen partial pressure on pyrite oxidation (Long, et al., 2004).

Parameters of experiment									
Temperature, ^{0}C							210		
d_{mean}, μm							62.6		
[FeS_2], g/L							1		
[H_2SO_4], M							0.5		
Results of experiment									
P_{O2}, kPa	1035			690			345		
Time, min	Conv., %	d/d_0	Fe^{3+}/Fe_{tot}	Conv., %	d/d_0	Fe^{3+}/Fe_{tot}	Conv., %	d/d_0	Fe^{3+}/Fe_{tot}
0	0.00	1.00	0.0	0.00	1.00	0.0	0.00	1.00	0.0
5	0.43	0.83	54.4	0.32	0.88	64.2	0.23	0.91	59.5
10	0.68	0.68	71.9	0.59	0.74	45.6	0.46	0.81	10.6
15	0.86	0.52	81.3	0.77	0.62	58.7	0.63	0.71	39.1
20	0.93	0.42	83.7	0.87	0.51	75.8	0.75	0.62	55.0
30	0.98	0.28	86.4	0.94	0.40	79.0	0.87	0.50	68.2
45	1.00	0.19	87.2	0.97	0.31	80.2	0.92	0.42	72.3
60	1.00	0.11	87.6			81.1	0.94	0.39	74.7
90			88.8			81.1	0.96	0.32	76.2
120			89.4			81.3	0.97	0.32	77.6